

# Determining the essentially different partitions of all Japanese convex tangrams

T.G.J. Beelen and T. Verhoeff (TU Eindhoven)

December 4, 2018

## Contents

<b>1 Abstract</b>	<b>3</b>
<b>2 General Introduction</b>	<b>4</b>
2.1 The relationships between the tans . . . . .	5
2.2 Problem formulation . . . . .	5
<b>3 Finding all layouts of the convex polygons with the Japanese tans</b>	<b>7</b>
<b>4 The Square tangram</b>	<b>8</b>
4.1 The case Tr1 . . . . .	8
4.2 The case Tr4 . . . . .	9
4.3 The cases Tr2, Tr3, Tr5 and Tr6 . . . . .	10
4.4 The cases Tr7 and Tr8 . . . . .	11
<b>5 The Strip tangram J14</b>	<b>14</b>
5.1 Preliminaries . . . . .	14
5.1.1 Visualisation aspects . . . . .	15
5.2 Finding all possible layouts of strip J14 . . . . .	18
5.2.1 The layouts of the strip with Tz1 and Tz2 . . . . .	18
5.2.2 The layouts of J14 with Tz1 . . . . .	19
5.2.3 The layouts of J14 with Tz2 . . . . .	19
5.2.4 The layouts of J14 with Tz3 . . . . .	21
5.2.5 The layouts of the strip with Tz3 . . . . .	22
5.2.6 Summary of the analysis of <i>Strip_J14</i> . . . . .	27
5.2.7 Strip J14 with its twin layouts . . . . .	29
5.3 Finding all different partitions for J15 and J16 by a combinatorial approach . . . . .	30

<b>6</b>	<b>An algorithm for generating all partitions of a convex shape</b>	<b>34</b>
6.1	A simple packing problem . . . . .	34
6.2	A more complicated packing problem . . . . .	37
6.2.1	The packing problem for <i>Strip J14</i> . . . . .	38
6.2.2	The packing problem for <i>Strip J16</i> . . . . .	38
<b>7</b>	<b>All different partitions of the shapes <i>J01</i> up to <i>J16</i></b>	<b>40</b>
<b>8</b>	<b>Acknowledgments and References</b>	<b>49</b>

## 1 Abstract

In this report we consider the set of the 16 possible convex tangrams that can be composed with the 7 so-called “Sei Shonagon Chie no Ita” (or Japanese) tans, see [10]. The set of these Japanese tans is slightly different from the well-known set of 7 Chinese tans with which 13 (out of those 16) convex tangrams can be formed. In [4], [6] the problem of determining all essentially different partitions of the 13 “Chinese” convex tangrams was investigated and solved. In this report we will address the same problem for the “Japanese” convex tangrams. The approach to solve both problems is more or less analogous, but the “Japanese” problem is much harder than the “Chinese” one, since the number of “Japanese” solutions is much larger than the “Chinese” ones. In fact, only for a few “Japanese” tangram shapes their solutions can be found by a rigorous analysis supported by a large number of clarifying diagrams. The solutions for the remaining shapes have to be determined using a dedicated computer program. Both approaches will be discussed here and all essentially different solutions with the “Japanese” tans are presented. As far as we know all presented results are not yet published before.

*Keywords:* tangram, partition, backtracking, visualization.

## 2 General Introduction

The word “tangram” is reasonably well-known, especially in the context of trying to compose a given figurative picture using 7 geometrically shaped puzzle pieces called tans. A few typical examples of such pictures are given in Fig. 1. Furthermore, in the bilingual (German / Dutch) book “Tangram, / Das alte chinesische Formenspiel / Het oude Chinese vormenspel ” by J. Elffers [2] over 1600 examples on tangram puzzles and their solutions can be found. See also website [6] <http://www.pentoma.de/>.

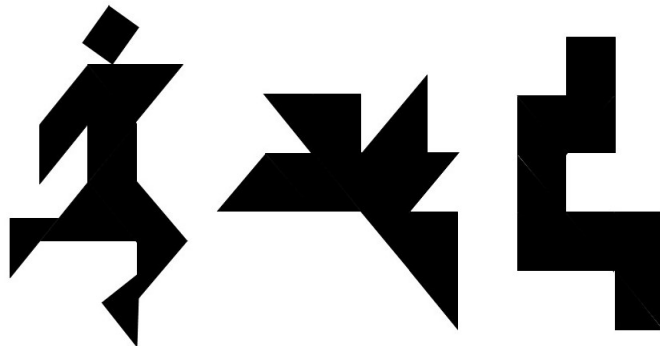


Figure 1: A few typical tangram figures.

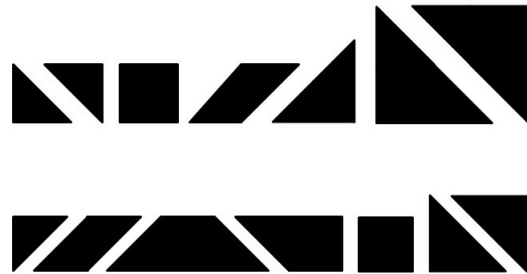


Figure 2: The 7 individual Chinese and the 7 Japanese tangram pieces, in the top and bottom row, respectively.

It should be noticed that next to the set of Chinese tans, there also exists a less known set of Japanese tans, in shape similar to the Chinese tans. Both the sets of Chinese and Japanese tans are shown in Fig. 2. Just as in case of the Chinese tans, each Japanese piece can be decomposed into one or more of the smallest triangular pieces. See Fig. 3.

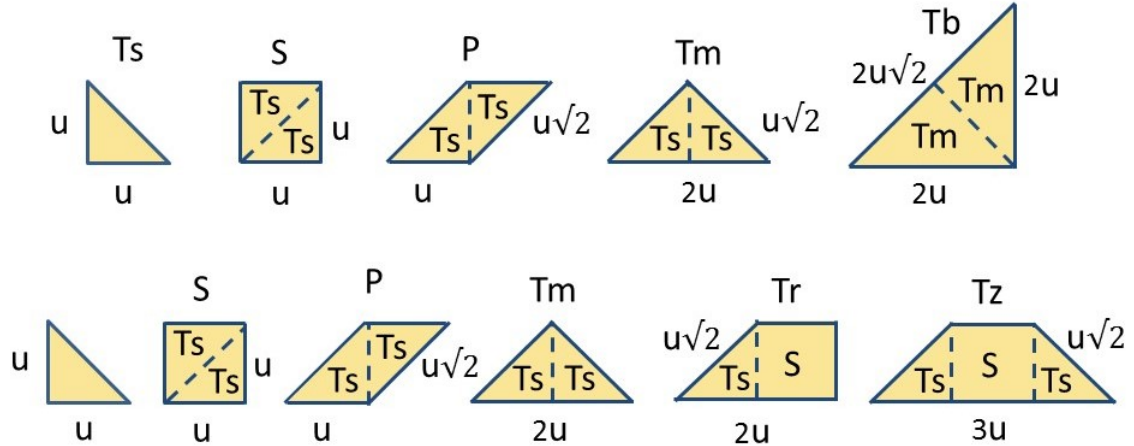


Figure 3: The composition of the Chinese (top row) and Japanese tans (bottom).

## 2.1 The relationships between the tans

Let us consider Figs. 2 and 3 in more detail. The set of Chinese tans consists of the following 7 pieces: one small triangle  $T_s$ , one square  $S$ , one parallelogram  $P$ , two medium sized triangles  $T_m$  and two big triangles  $T_b$ .

The set of Japanese tans also consists of 7 pieces: one small triangle  $T_s$ , one square  $S$ , one parallelogram  $P$ , two medium sized triangles  $T_m$  (exactly as in the Chinese set), one rectangular trapezium  $T_r$  and one isosceles trapezium  $T_z$ . Notice that the Chinese and Japanese tans  $T_s$ ,  $S$ ,  $P$  and  $T_m$  are identical.

The relationship between the areas of the tans is indicated in Fig. 3.

**Relationships between the tans :** (1)

- (i)  $S = 2 T_s$  ,  $P = 2 T_s$  ;
- (ii)  $T_m = 2 T_s$ ,  $T_b = 2 T_m = 4 T_s$  ;
- (iii)  $T_r = T_s + S = 3 T_s$ ,  $T_z = 2 T_s + S = T_r + T_s = 4 T_s$  ;
- (iv) Tangram with all 7 Chinese tans  $= 2 T_b + T_m + 2 T_s + S + P = 16 T_s$  ;
- (v) Tangram with all 7 Japanese tans  $= T_z + T_r + 2 T_m + T_s + S + P = 16 T_s$  ;

## 2.2 Problem formulation

For convenience, let us denote the above mentioned sets of Chinese and Japanese tans by  $Tans\_C$  and  $Tans\_J$ , respectively. It is immediately clear that we can create a huge number of tangrams that can be composed using either the set  $Tans\_C$  or  $Tans\_J$ . In 1942 two Chinese mathematicians Fu Traing Wang and Chuan-Chih Hsiung published a paper [1] dealing with the problem of finding all *convex* polygons in 2D. They showed that there exist precisely 20 convex polygons, see Fig. 4. Here the numbering is conform to that in [1] as follows. The shapes marked by \* in their

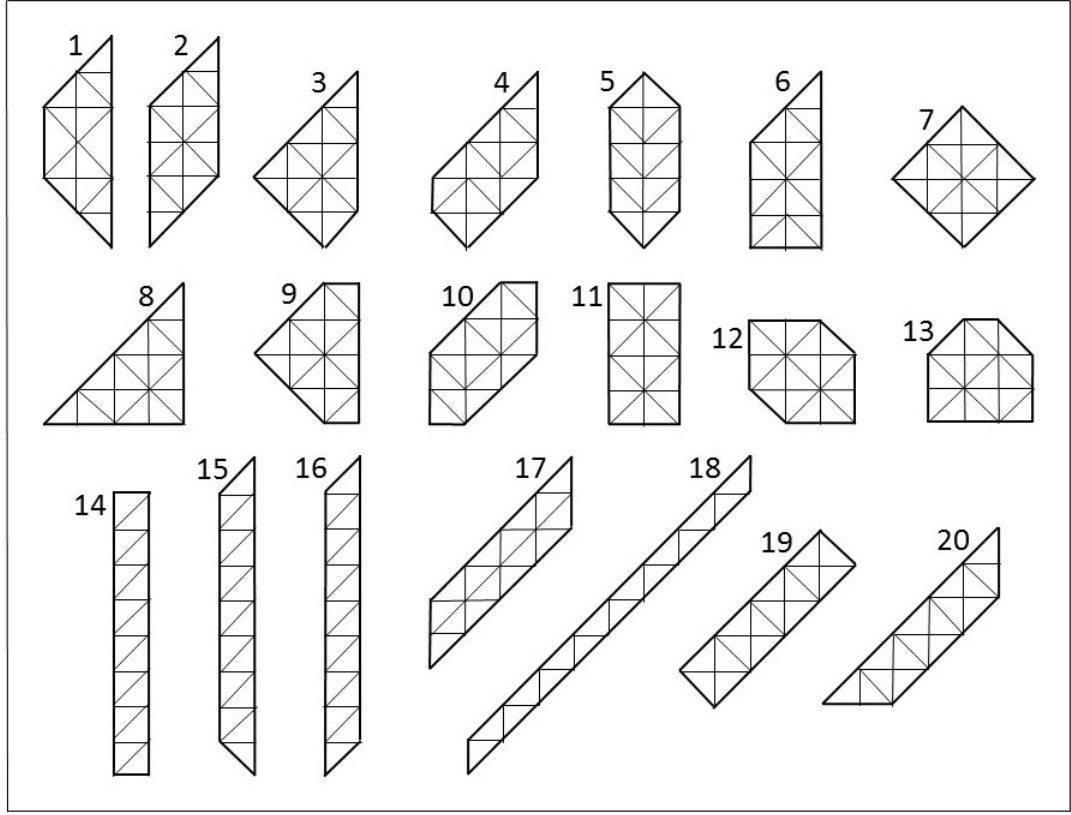


Figure 4: All 20 convex polygons.

table correspond to the numbers 14-16, while the 13 unmarked shapes as listed in their order are numbered 1-13 here. Clearly, these 13 shapes can be covered by the set  $C\_tans$  and they will be denoted by the set  $Poly13$ .

Notice that all 20 polygons can be formed by 16 rectangular isosceles triangles, as shown in Fig. 4. In 2014 it was shown by Eli Fox-Epstein and Ryunhei Uehara [10] that even 3 more (so in total 16, but not more) convex polygons can be covered by using the set  $J\_tans$ , being the shapes 14-16 in Fig. 4. We will call the polygons 1-16 the set  $Poly16$  (thus  $Poly16 \supset Poly13$ ). Moreover, it was also shown in [10] that more coverings are possible, but then different tan sets must be used.

A mathematically interesting question on tangram covering is how many essentially different partitions for all polygons in  $Poly13$  and  $Poly16$  exist. In [3] this problem was extensively analyzed and solved for  $Poly13$  with the set  $C\_tans$ .

In this report we will address the covering problem for  $Poly16$  with the set  $J\_tans$ .

**Terminology :** In the rest of this report we will use the words *layout*, *partition*, *filling* and *covering* as synonyms.

### 3 Finding all layouts of the convex polygons with the Japanese tans

In this section we will give an overview of a few approaches we have chosen to solve the problem of finding all essentially different layouts with the Japanese tans (in short, to solve “The problem”). First we notice that solving this problem can be done by the well-known backtracking technique [8], [9], in a similar way as done in case of the Chinese tans (see [4]).

However, after proceeding manually as in [4] for a few “simple” tangrams it became clear that this would be a very tedious job for almost all convex shapes. So, an alternative was to carry out a backtracking algorithm by a computer. We will address this approach in section 6. In fact, we will discuss the following approaches to solve (partly or fully) “The problem”.

- (1) A systematic analysis of all possible partitions for the full square tangram, i.e. tangram 7 in Fig. 4.
- (2) A systematic analysis of all possible partitions for the rectangular strips (see shapes 14 up to 16 in Fig. 4, which will be indicated by  $J14$ ,  $J15$  and  $J16$  in the rest of this report). This analysis is done via backtracking and visualizing all possible trees. Notice that due to the length of the analyses of  $J15$  and  $J16$ , this is not included here, but can be found in [5].
- (3) An alternative ‘combinatorial’ approach for the strips  $J14$ ,  $J15$  and  $J16$ .
- (4) A global description of an algorithm to solve a so-called packing problem. We will explain how this algorithm can be used to solve “The Problem”. Moreover, all solutions (partitions and their number) of all 16 convex shapes are included.

## 4 The Square tangram

We start with adding the rectangular trapezium  $\text{Tr}$  to the empty tangram *Square*. Since *Square* is symmetric w.r.t. both its horizontal and vertical centerline we can restrict ourselves to placing  $\text{Tr}$  in the lower half of *Square*. See Fig. 5. We will discuss several cases in the next sections.

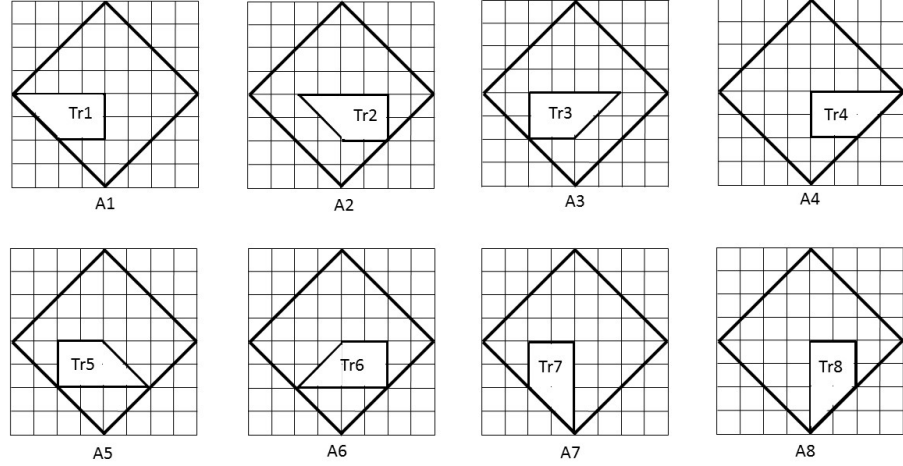


Figure 5: All possible layouts for tan  $\text{Tr}$  in the lower half of tangram *Square*

### 4.1 The case $\text{Tr1}$

Let us first consider the case with  $\text{Tr1}$ , see Fig. 5-A1. Clearly, we can add the isosceles trapezium  $\text{Tz}$  on 4 different positions as shown in Fig. 6. Next we can add the square  $\text{S}$  to these 4 layouts.

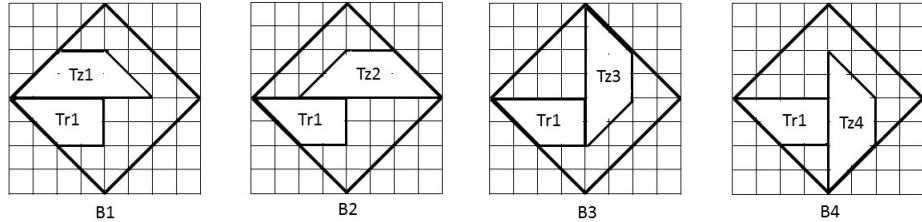


Figure 6: All possible combinations when adding  $\text{Tz}$  to  $\text{Tr1}$  in *Square*

Clearly, we have only one possibility for  $\text{S}$  per layout. See Fig. 7. However, the layouts C3 and C4 are not feasible since 2 tans  $\text{Ts}$  are needed (but not available) for a full covering of the square.

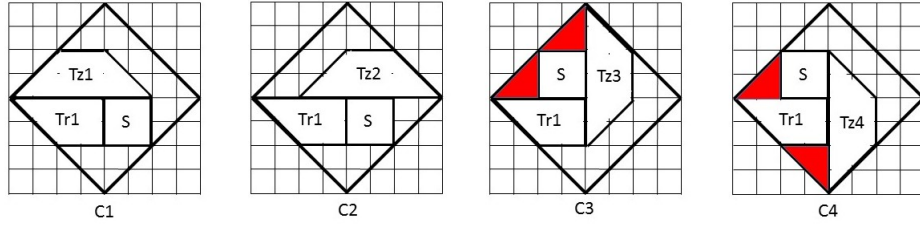


Figure 7: All possible combinations when adding S to Tr1.Tz in *Square*

So we have

**Conclusion:** (2)

The *Square* tangram has 2 potentially feasible layouts C1 and C2 with Tr1 and Tz.

#### 4.2 The case Tr4

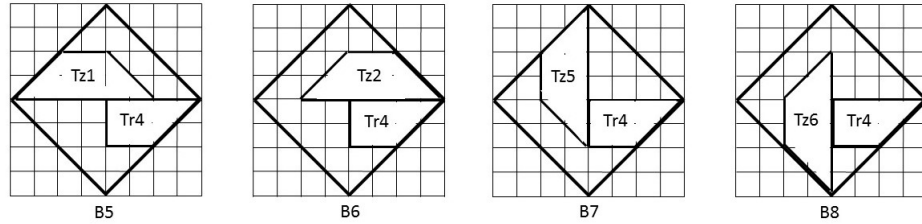


Figure 8: All possible combinations when adding Tz to Tr4 in *Square*

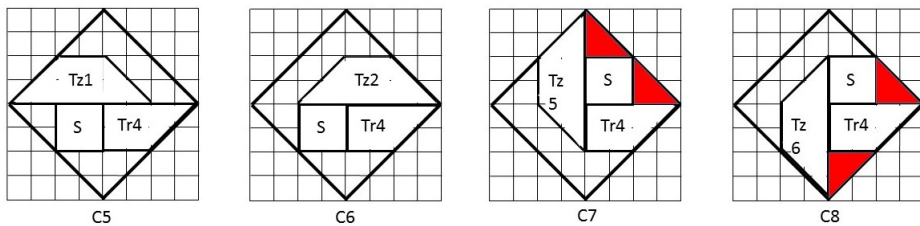


Figure 9: All possible combinations when adding S to Tr4.Tz in *Square*

In a similar way as in case Tr1 we can proceed with case Tr4. Indeed, here again we find 4 different combinations for Tr4 and Tz as shown in Fig. 8. Next we can add S to these 4 layouts, see Fig.9.

Similarly to case Tr1 the layouts C7 and C8 for Tr4 are not feasible. So we have

**Conclusion:** (3)

**The Square tangram has 2 potentially feasible layouts C5 and C6 with Tr4 and Tz.**

When comparing the potentially feasible layouts in Figs. 6 and 8 we see that the cases C1 and C6 as well as C2 and C5 are *equivalent* (by symmetry w.r.t. the vertical centerline of *Square*). Thus,

**Conclusion:** (4)

**We have to investigate the cases C1 and C2 further, but  
we can skip the cases C5 and C6 with Tr4.**

Before doing this, we first turn to the cases with Tr2, Tr3, Tr5 and Tr6.

### 4.3 The cases Tr2, Tr3, Tr5 and Tr6

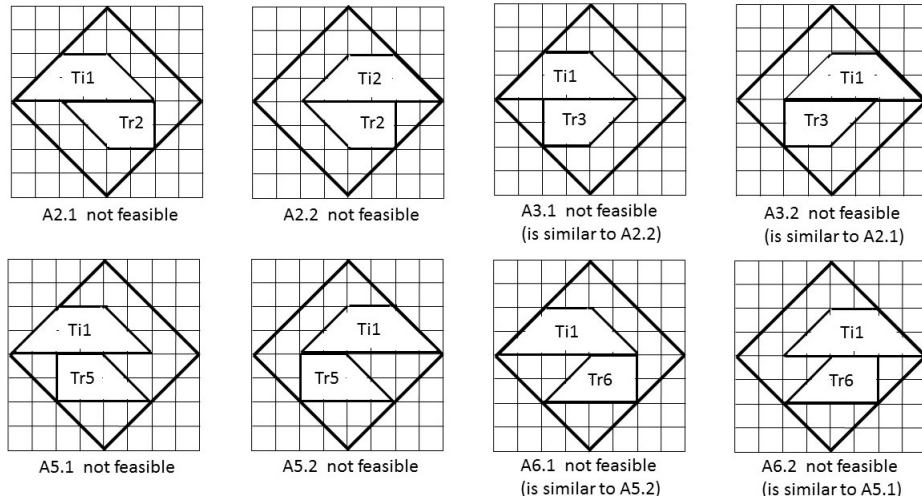


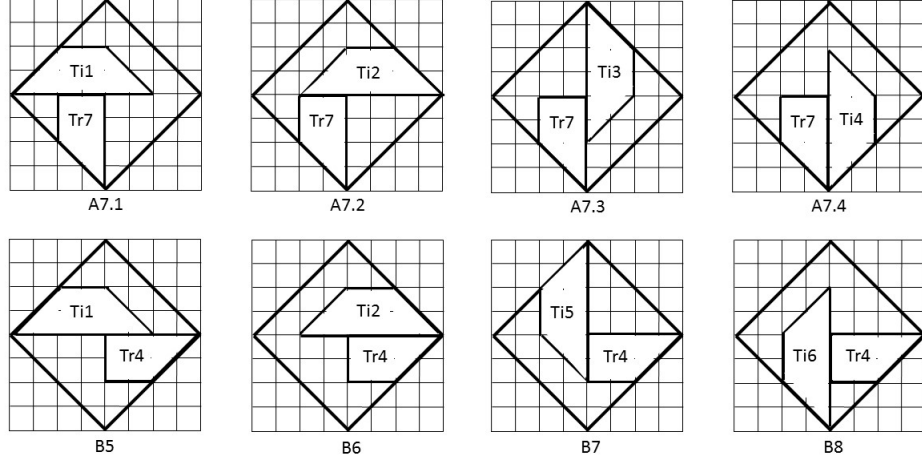
Figure 10: All possible combinations when adding Tz to Tr2, Tr3, Tr5 and Tr6 in *Square*

In Fig. 10 all possible cases with Tr2, Tr3, Tr5 and Tr6 are shown. It is easily seen that in all cases we cannot add the square tan S anymore. So, have

**Conclusion:** (5)

**The cases Tr2, Tr3, Tr5 and Tr6 are not feasible.**

Finally, we want to study the cases with Tr7 and Tr8.



Rotate each square  $A7.x$  over  $+90^\circ$ . Then  
 $A7.1 \equiv B8$ ,  $A7.2 \equiv B7$ ,  $A7.3 \equiv B5$ ,  $A7.4 \equiv B6$ . Thus,  
 $Tr7.Ti \equiv Tr4.Ti$ . So, we can ignore the partitions with  $Tr7$ .

Figure 11: All possible combinations when adding  $Tz$  to  $Tr7$  as well as to  $Tr4$  in *Square*

#### 4.4 The cases $Tr7$ and $Tr8$

In Fig. 11 all 4 possible cases for  $Tr7$  in *Square* are shown. Furthermore, the 4 possible cases for  $Tr4$  are repeated here (recall Fig.8). It can easily be seen that by rotating each configuration *Square.Tr7.Tz* over  $90^\circ$  we find one of the configurations with *Square.Tr4.Tz*. We call such a pair *equivalent* and this will be denoted by the symbol  $\equiv$ . Specifically, in Fig. 11 we have  $A7.1 \equiv B8$ ,  $A7.2 \equiv B7$ ,  $A7.3 \equiv B6$  and  $A7.4 \equiv B5$ . Hence, we have

**Conclusion:** (6)

**We can ignore all partitions with  $Tr7$  for further study (and continue with  $Tr4$ ).**

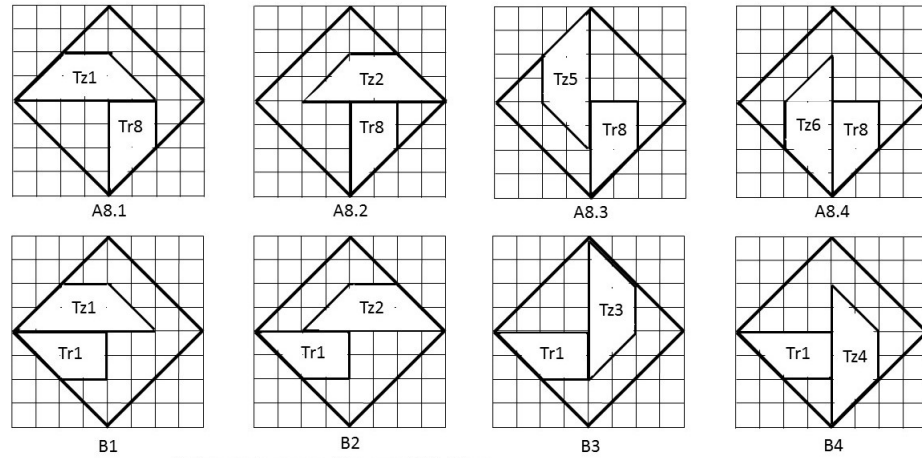
Let us now consider case *Square.Tr8*.

In Fig. 12 all 4 possible cases for *Square.Tr8* are shown. Moreover, for easy comparison we also recall the 4 possible cases for  $Tr1$  from Fig.6. It can easily be seen that by rotating each configuration *Square.Tr8.Tz* over  $90^\circ$  we find one of the configurations with *Square.Tr1.Tz*. Specifically, we have  $A8.1 \equiv B3$ ,  $A8.2 \equiv B4$ ,  $A8.3 \equiv B2$  and  $A8.4 \equiv B1$ . Hence, we have

**Final Conclusion:** (7)

**We can ignore all partitions with  $Tr8$  for further study (and continue with  $Tr1$ ).**

Combining all conclusions (2) up to (7) above we see that we only need to investigate the layouts C1 and C2 in Fig. 7 for yes/no feasibility.



Rotate each square A8.x over  $-90^\circ$ . Then  
 $A8.1 \equiv B3$ ,  $A8.2 \equiv B4$ ,  $A8.3 \equiv B5$ ,  $A8.4 \equiv B6$ . Thus,  
 $Tr8.Tz \equiv Tr1.Tz$ . So, we can ignore the partitions with  $Tr8$ .

Figure 12: All possible combinations when adding  $Tz$  to  $Tr8$  as well as to  $Tr1$  in *Square*

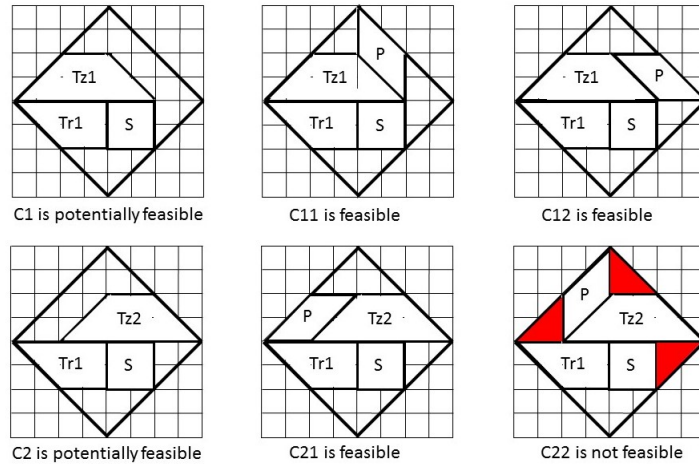


Figure 13: All possible combinations when adding  $P$  to  $Tr1.Tz.S$  in *Square*

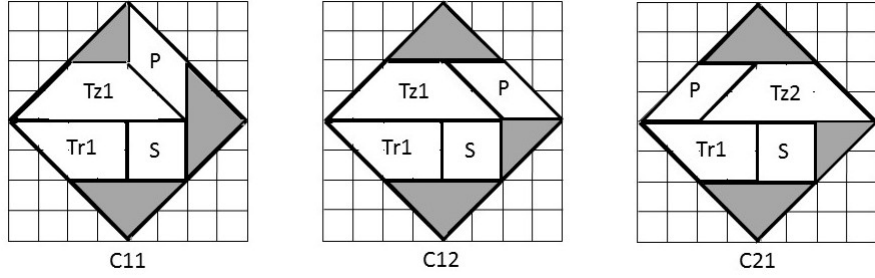


Figure 14: The 3 feasible partitions for *Square*

Therefore, we return to the layouts C1 and C2 in Fig. 7. Let us try to add parallelogram P to them, see Fig.13. Clearly, we have 2 options for adding P to *Square\_Tr1.Tz1.S*, see Figs. 13-C11, C12. Clearly, after having added P we see that 3 empty regions are left in both C11 and C12, and they can be uniquely be covered by the triangles Tm1, Tm2 and Ts. Notice that the order of placing Tm1 and Tm2 is irrelevant. Thus, layout *Square\_Tr1.Tz1.S* can be completed in two different ways to a full feasible covering of *Square*.

Similarly to C1 we can add P to *Square\_Tr1.Tz2.S*, but now only one layout (C21) is feasible, since in the other one (C22) we cannot add both triangles Tm1 and Tm2. See Figs. 13-C21, C22. So, we have

**Final Conclusion:** (8)

**Square  $Tr1.Tz1.S$  can be fully covered by 3 different layouts, see Fig. 14.**

## 5 The Strip tangram J14

We start by giving some preliminaries.

### 5.1 Preliminaries

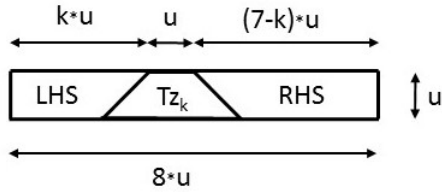


Figure 15: Trapezium  $Tz$  with its LHS and RHS parts in strip  $J14$ .

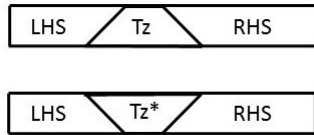


Figure 16: Equivalence of the strips with  $Tz$  and  $Tz^*$  ( $= Tz$  upside-down) in  $J14$

Since  $Tz$  is an isosceles trapezium in a rectangular strip, we need to add tans at the left (LHS) as well as at the right hand side (RHS) of  $Tz$ . See Fig.15. Clearly, to each side of  $Tz$  we have to add a *skew*-sided tan. Notice that the subscript  $k$  in the name  $Tz_k$  refers to the length of LHS. Furthermore, notice that each strip with  $Tz$  is equivalent to the strip with  $Tz$  upside-down (due to symmetry w.r.t. the bottom edge of the strip). See Fig.16.

Let us now consider all possible positions of  $Tz$  in the strip, see Fig.17. The strips will be identified by the  $Tz$  name. It is easily seen (by reflection w.r.t. the vertical left hand edge of the strip) that the following strips are equivalent:  $Tz_4 \equiv Tz_3$ ,  $Tz_5 \equiv Tz_2$  and  $Tz_6 \equiv Tz_1$ .

Thus, we need not to generate layouts with  $Tz_4$  up to  $Tz_6$ .

So, we have

**Conclusion:** (9)

**We only need to find all possible different layouts of the strip  $J15$   
with  $Tz_1$  up to  $Tz_3$  (see Fig. 17).**

Consider Fig. 15 for  $k = 1, 2, 3$ . In Figs. 18 and 19 we show all possible fillings for LHS corresponding to  $Tz_k$ . Clearly, once knowing all possible fillings for LHS and RHS we can find all different layouts of a partial strip  $J14$  for each feasible combination of LHS and  $Tz$  (using Figs. 4 and 5) by adding step by step one tan from the set of remaining pieces. This can be done in a

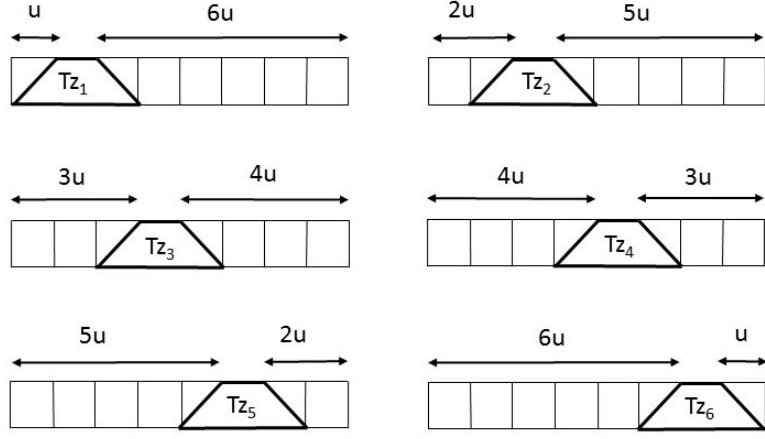


Figure 17: All possible positions of  $Tz$  in the strip.

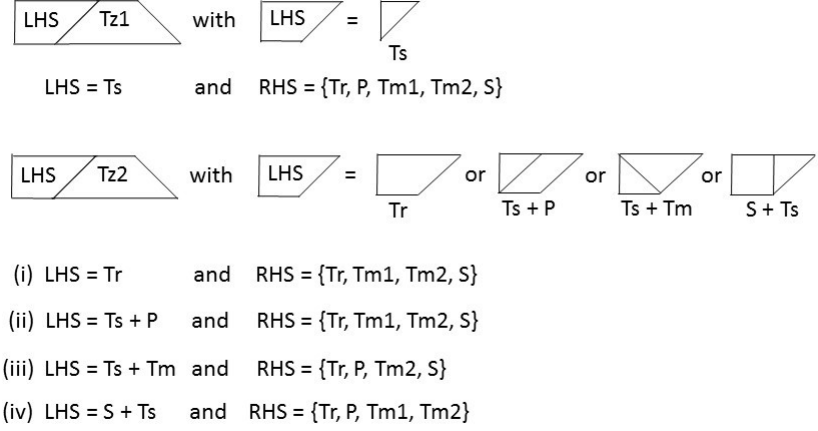


Figure 18: All fillings for LHS and Tz1 and Tz2 in *Strip\_J14*.

well-defined way by using the so-called backtracking procedure [8], [9]. Below we will give more details.

However, we first want to explain a few notational and visualization aspects.

### 5.1.1 Visualisation aspects

We start with a partial strip  $LHS + Tz$  and add a suitable tan (called  $T1$  for simplicity) next to  $Tz$ . We get the (partial) strip  $LHS + Tz + RHS = LHS + Tz + T1$ . Notice that there are 2 options for each tan to be added: either the tan fits to the strip in a unique way or the tan does not fit at all.

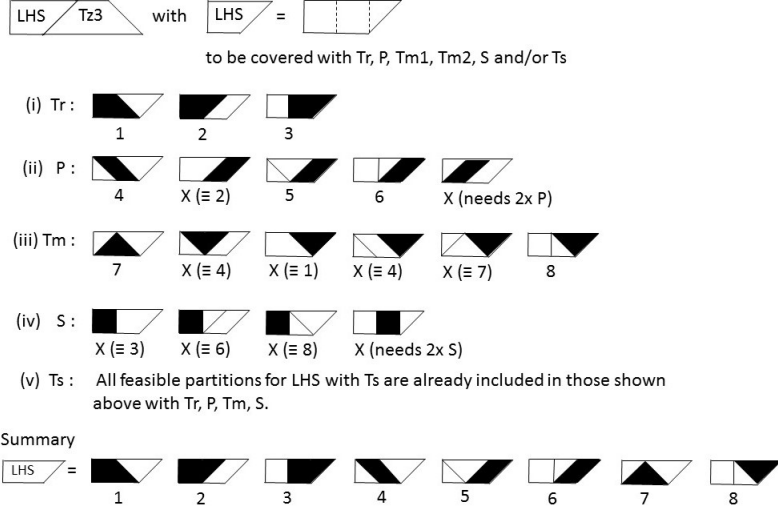


Figure 19: All fillings for LHS and Tz3 in *Strip\_J14*.

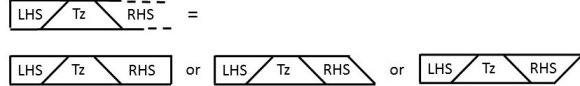


Figure 20: The 3 possible rhs-edges of a partial *Strip\_J14*.

Clearly, the rhs-edge of each partial strip is vertical, left- or right skew, see Fig. 20 and the final strip must have a vertical rhs-edge. By adding more tans  $T_2, T_3, \dots$  the size of the strip grows. This process can be visualized by a tree structure. It is easily seen that the tree will grow widely when showing all partial strips in full detail. However, we will show not all details but only the actual strip globally.

We will clarify this by the following representative example.

### Visualisation of the backtracking process

Consider Fig. 21 where we have a partial strip  $S_0 = LHS + T_z$  with  $LHS = T_s + P$ .

Then the remaining tans are  $Tr, Tm1, Tm2$  and  $S$  and these names are listed under  $S_0$ . We can extend  $S_0$  with either  $Tr$  or  $Tm$ , resulting in the partial strips  $S_{1.1}$  and  $S_{1.2}$ , respectively.

Clearly,  $S_{1.1}$  is fully rectangular while  $S_{1.2}$  has a skew rhs-edge. The remaining tans for extending  $S_{1.1}$  are  $Tm1, Tm2$  and  $S$  (these names are listed under  $S_{1.1}$ ). However,  $S_{1.1}$  can only be extended with  $S$ , resulting in  $S_{2.1}$ , with  $Tm1$  and  $Tm2$  left. It is easily seen that these tans cannot be used anymore for extending  $S_{2.1}$ . This fact is indicated by  $X$  in the figure and this branch of the tree ends here. So, adding the tans in this order does not result in a full strip.

On the other hand, when first adding one of the triangles  $Tm1$ ,  $Tm2$  (say  $Tm1$ ) to  $S0$  we find the

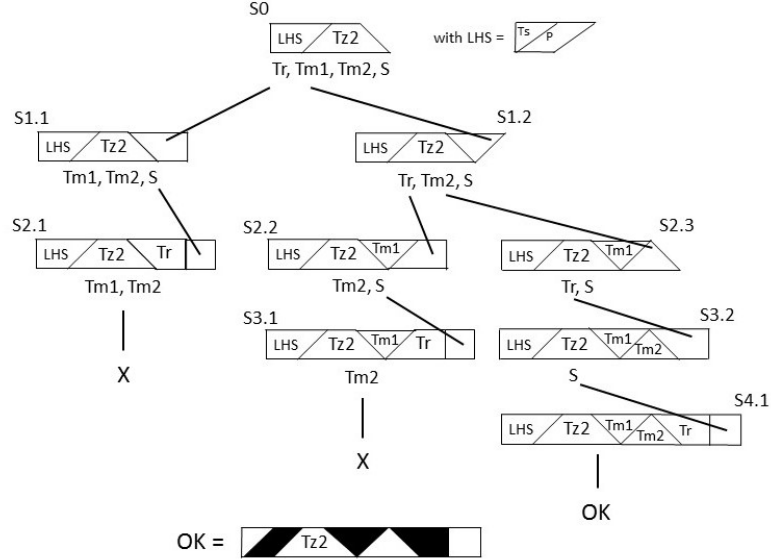


Figure 21: Example of a tree structure for finding all layouts of the strip J14.

strip  $S1.2$ , which can be extended by adding either  $Tr$  or  $Tm2$ , resulting in the strips  $S2.2$  and  $S2.3$ , respectively. Now the remaining tans for extending  $S2.2$  are  $Tm2$  and  $S$  (see below  $S2.2$ ), but only  $S$  can be added, resulting in  $S3.1$ . However,  $S3.1$  cannot be extended further, again indicated by  $X$  and this branch also ends.

Let us now consider  $S2.3$ . Here the remaining tans for extension are  $Tr$  and  $S$ . Clearly,  $S2.3$  can be extended with only  $Tr$ , giving strip  $S3.2$  and tan  $S$  is left. Finally,  $S3.2$  can be extended by  $S$ , giving a final full strip, indicated by  $OK$ . The structure of the final full strip is also given.

### Simplification of the tree visualization

It should be noticed that in fact we do not need to know the full filling details of the intermediate partial strips. Indeed, only the overall shape of each partial strip is relevant for finding a possible extension. So, we can replace the detailed scheme above by a more global scheme, as shown in Fig. 22-left. We emphasize that in this tree at each level (except top level) we have only indicated (in black) the *global* shape (and actual) size of the partial strip in the previous level. However, the newly added tan at the current level is shown with its *actual* shape and *actual* size.

Finally, we even can reduce the width of the figure a bit more by using the *same* size for all partial strips, but preserving their global shape, as shown in Fig. 22-right.

In all next figures we will only use the latter compact visualization.

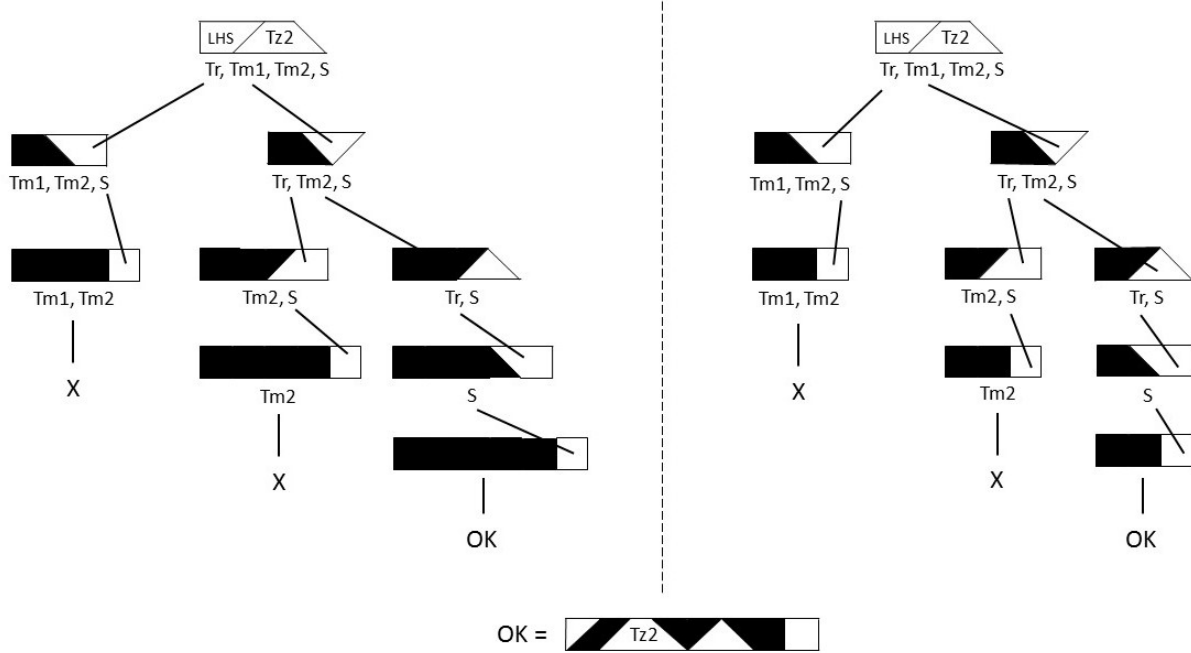


Figure 22: Two global visualizations of a tree structure for J14.

## 5.2 Finding all possible layouts of strip J14

### 5.2.1 The layouts of the strip with Tz1 and Tz2

As indicated in Fig. 18 we see that (i) in case of Tz1 the corresponding LHS consists of one single tan, being Ts, and (ii) in case of Tz2 that LHS consists of one or two tans. All layouts for J14 with Tz1 and Tz2 are given in Figs. 23 up to 27.

### 5.2.2 The layouts of J14 with $Tz1$

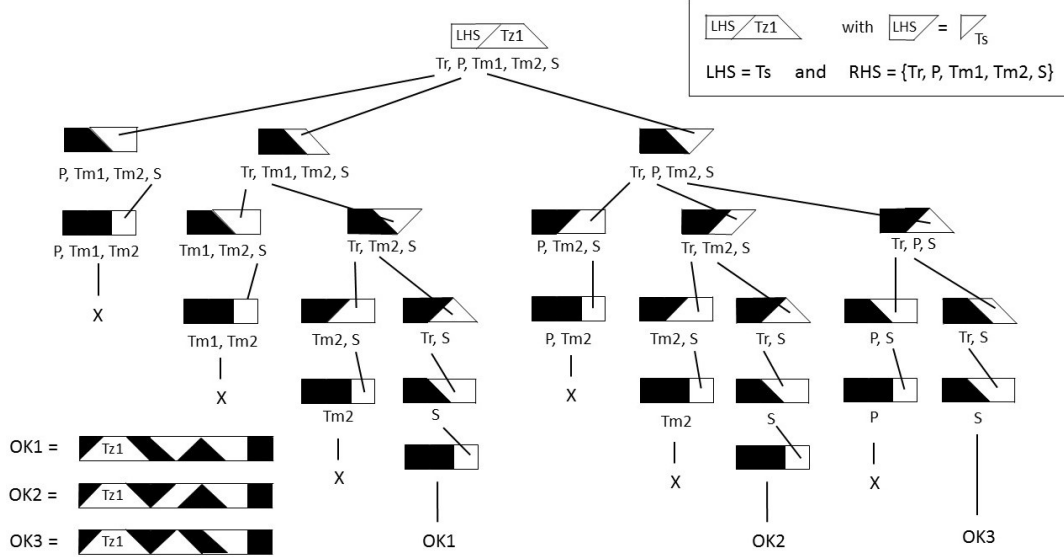


Figure 23: Visualization of Strip J14-Tz1.

### 5.2.3 The layouts of J14 with $Tz2$

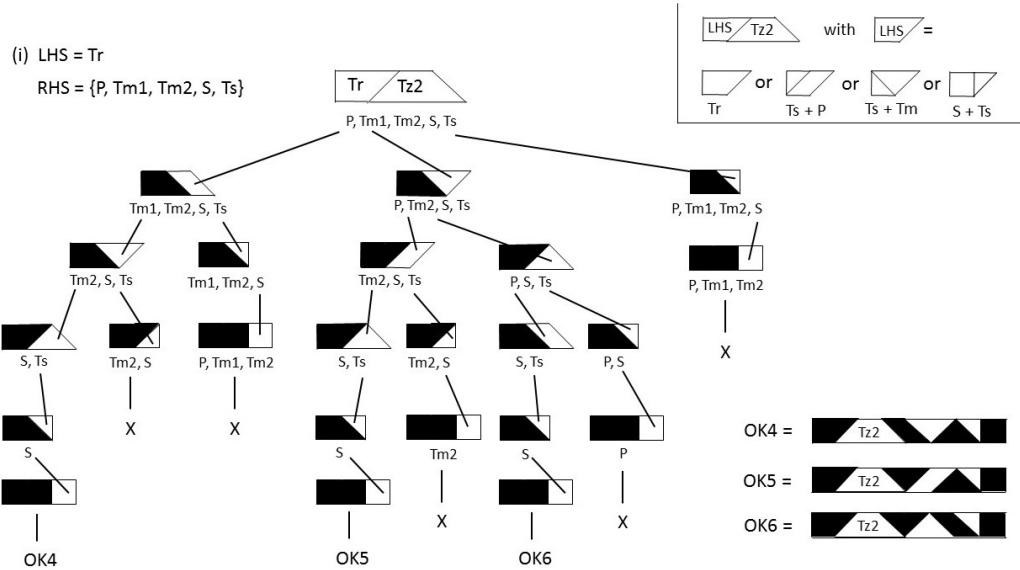


Figure 24: Visualization of Strip J14-Tz2.1.

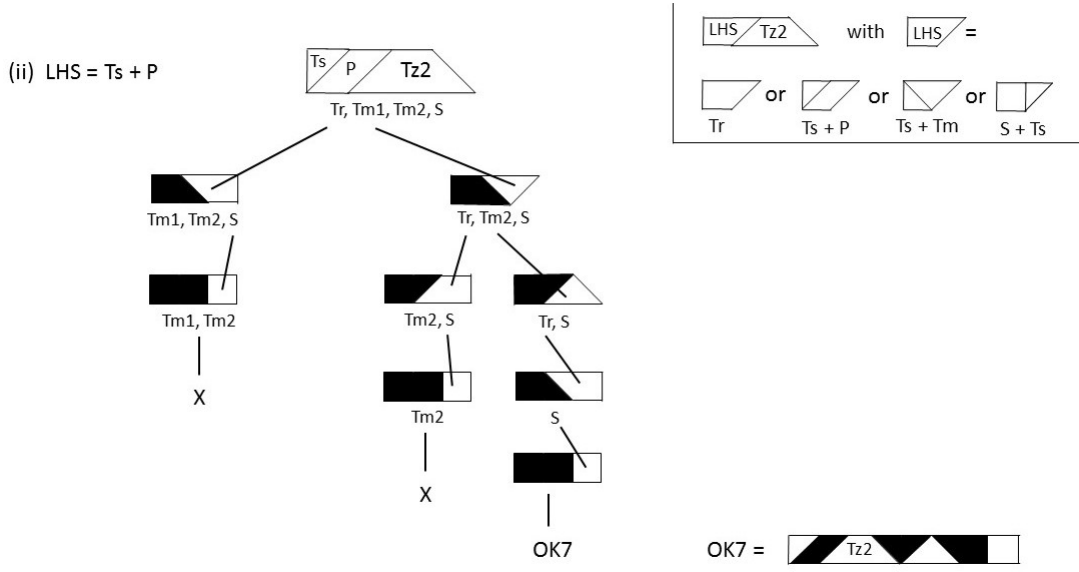


Figure 25: Visualization of Strip  $J14\_Tz2.2$ .

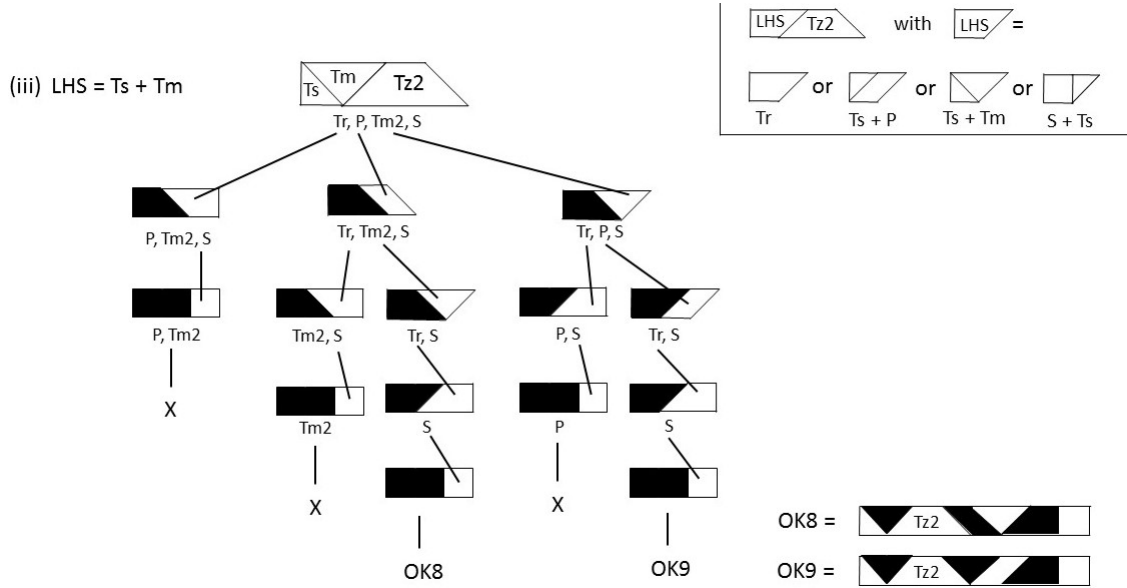


Figure 26: Visualization of Strip  $J14\_Tz2.3$ .

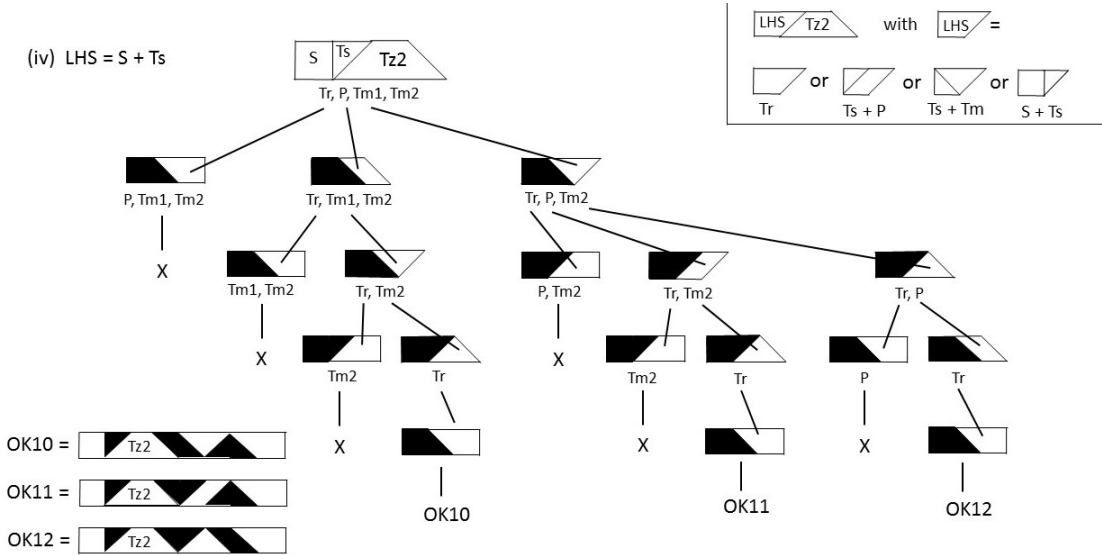


Figure 27: Visualization of Strip  $J14\_Tz2.4$ .

#### 5.2.4 The layouts of $J14$ with $Tz3$

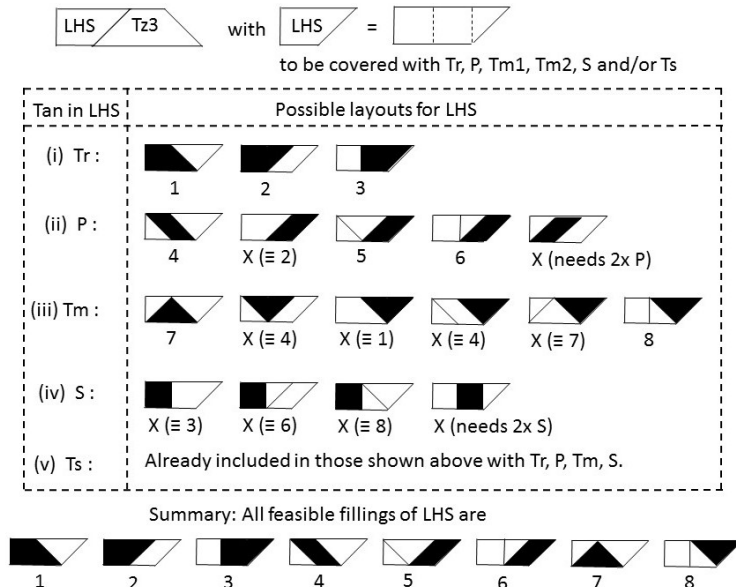


Figure 28: Investigation of the LHS partitions of Strip  $J14\_Tz3$ .

### 5.2.5 The layouts of the strip with Tz3

As indicated in Fig. 28 we see that in case of Tz3 the corresponding LHS consists of 2 or 3 tans, resulting in 8 feasible fillings. Notice that the left-edge of LHS is vertical, to be realized by one of the 3 tans Tr, S and Ts. Further, RHS has a skew left edge and a vertical right edge. The latter must also be realized by one of the 3 tans Tr, S and Ts. So, when fixing one of these 3 for realizing the vertical edge of LHS, at most 2 of them are left for building RHS.

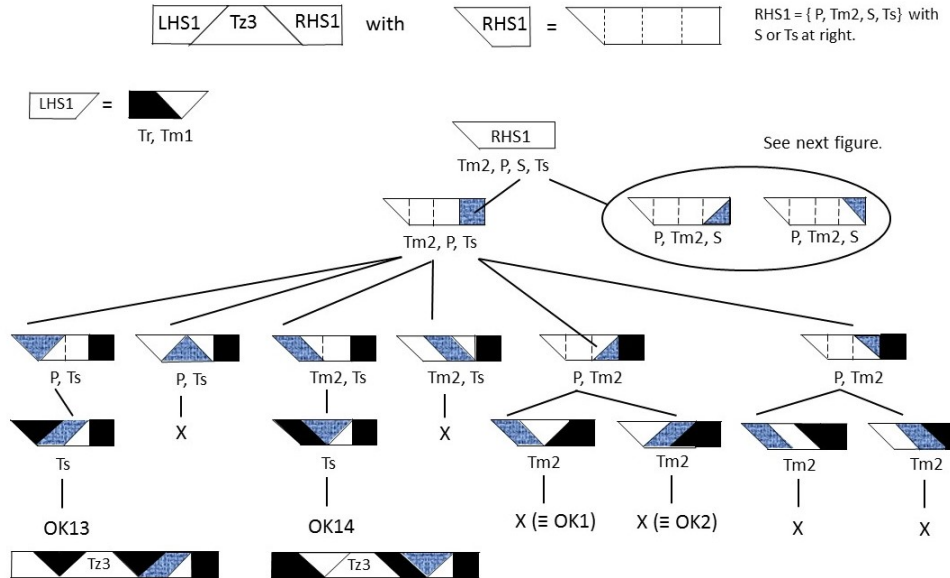


Figure 29: Investigation of Strip J14-Tz31, part (i).

In Figs. 29 and 30 we show the partial fillings of RHS ending at right with S or Ts. Clearly, Fig. 29 is self-explaining.

Fig. 30 shows the fillings of RHS ending at right with Ts. Next, after having added S in the 4 RHS-strips we still need to add P and Tm. However, for a full filling of all these 4 sub-strips we need an additional tan Ts, but this is not available. Thus, this branch of the tree does not end with a feasible filling of RHS.

Figs. 31 and 32 are also self-explaining.

In Fig. 33 we show the partial fillings of RHS4 ending at right with Tr or S. In Fig. 34 we consider the case where LHS5 consists of the same tans (Ts, P and Tm1) as in the previous figure. Consequently, RHS5 is identical to RHS4 since the same tans for RHS5 are available as for RHS4. However, since LHS5 has a partition being different from that of LHS4, we find with LHS5, Tz3 and RHS5 a different partition of the whole strip which is different from that in the previous case with LHS4, Tz3 and RHS4.

$\boxed{\text{LHS1}} \quad \boxed{\text{Tz3}} \quad \boxed{\text{RHS1}}$  with  $\boxed{\text{RHS1}} = \boxed{\text{RHS1}}$

$\text{RHS1} = \{ P, Tm2, S, Ts \}$  with  
S or Ts at right.

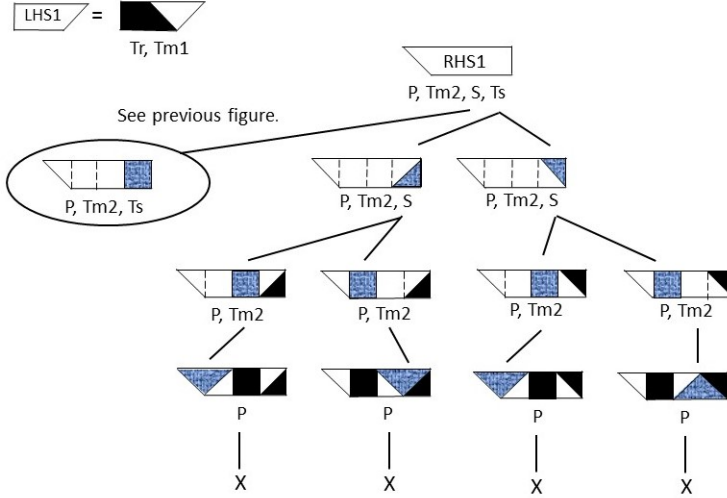


Figure 30: Investigation of Strip J14-Tz31, part (ii).

In Fig. 35 we consider the case LHS6 with Tr, Tm1 and Tm2. Since both triangles do not have a vertical edge we have to place Tr at right, resulting in 2 layouts. Clearly, only one feasible partition can be made with Tm1 and Tm2.

$LHS2 \diagup Tz3 \diagdown RHS2$  with  $\begin{array}{c} \diagup \\ LHS2 \end{array} = \begin{array}{c} \diagup \\ \square \end{array}$   $\begin{array}{c} \diagdown \\ RHS2 \end{array} = \begin{array}{c} \diagdown \\ \square \end{array}$   $RHS2 = \{ Tm1, Tm2, S, Ts \}$   
with S or Ts at right.

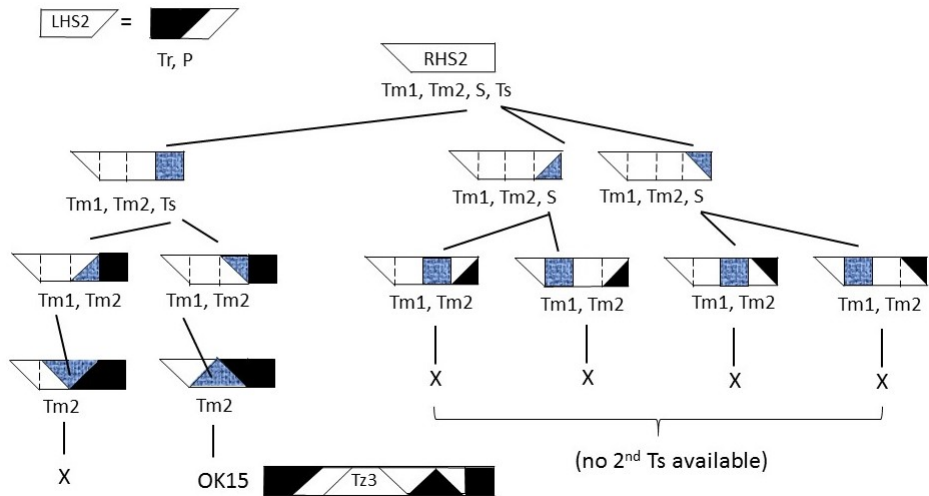


Figure 31: Investigation of Strip  $J14\_Tz32$ .

$LHS3 \diagup Tz3 \diagdown RHS3$  with  $\begin{array}{c} \diagup \\ LHS3 \end{array} = \begin{array}{c} \diagup \\ \square \end{array}$   $\begin{array}{c} \diagdown \\ RHS3 \end{array} = \begin{array}{c} \diagdown \\ \square \end{array}$   $RHS3 = \{ P, Tm1, Tm2, Ts \}$   
with S or Ts at right.

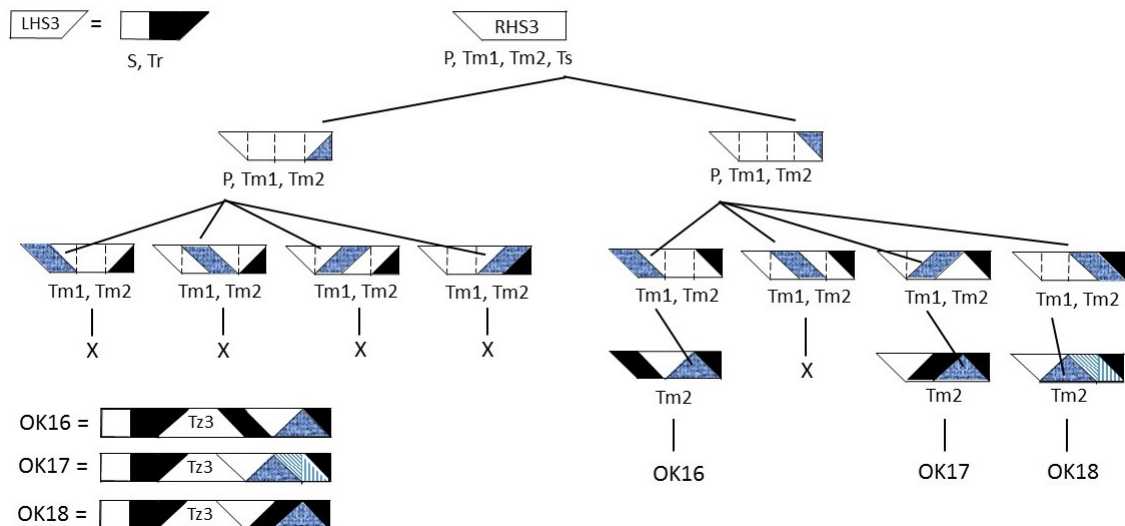


Figure 32: Investigation of Strip  $J14\_Tz33$ .

$$\boxed{\text{LHS4} \quad \text{Tz3} \quad \text{RHS4}} \quad \text{with} \quad \boxed{\text{RHS4}} = \boxed{\text{Tr} \quad \text{Tm2} \quad \text{S}}$$

RHS4 = { Tr, Tm2, S }  
With Tr or S at right.

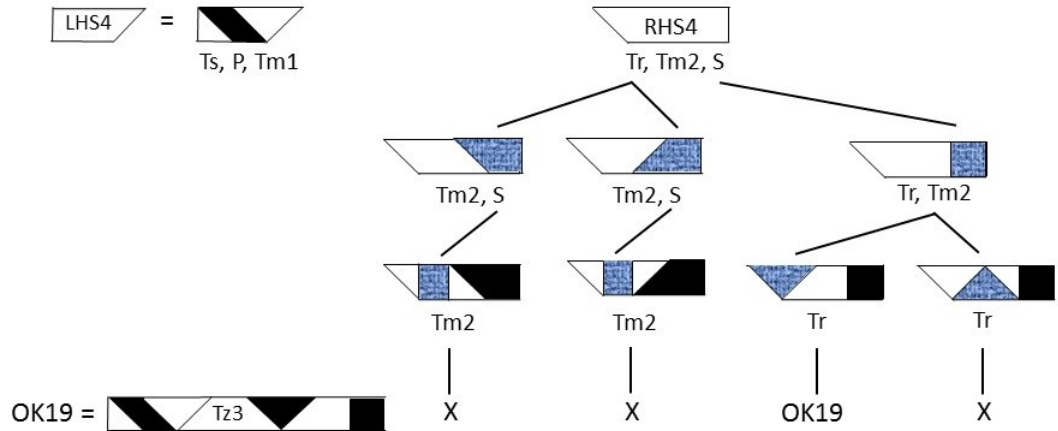


Figure 33: Investigation of Strip J14\_Tz3.4.

$$\boxed{\text{LHS5} \quad \text{Tz3} \quad \text{RHS5}} \quad \text{with} \quad \boxed{\text{RHS5}} = \boxed{\text{Tr} \quad \text{Tm2} \quad \text{S}} = \{ \text{Tr, Tm2, S} \}$$

$$\boxed{\text{LHS5}} = \boxed{\text{Ts, Tm1, P}} \quad \boxed{\text{RHS5}} = \boxed{\text{Tr, Tm2, S}}$$

This case is identical to RHS-4, since here the same tans are available for covering as in RHS4.  
So, RHS5 = RHS4. However, since LHS-4 is different from LHS-5, we do have a new different partition of the whole strip. It is labeled as OK20.

$$\begin{aligned} \text{OK20} &= \boxed{\text{LHS5} \quad \text{Tz3} \quad \text{RHS5}} \\ &= \boxed{\text{Ts, Tm1, P} \quad \text{Tz3} \quad \text{Tr, Tm2, S}} \end{aligned}$$

Figure 34: Investigation of Strip J14\_Tz3.5.

$$\boxed{\text{LHS6}} \diagup \text{Tz3} \diagdown \boxed{\text{RHS6}} \quad \text{with} \quad \boxed{\text{RHS6}} = \begin{array}{c} \diagup \\ \diagdown \end{array} \quad = \{ \text{Tr}, \text{Tm1}, \text{Tm2} \}$$

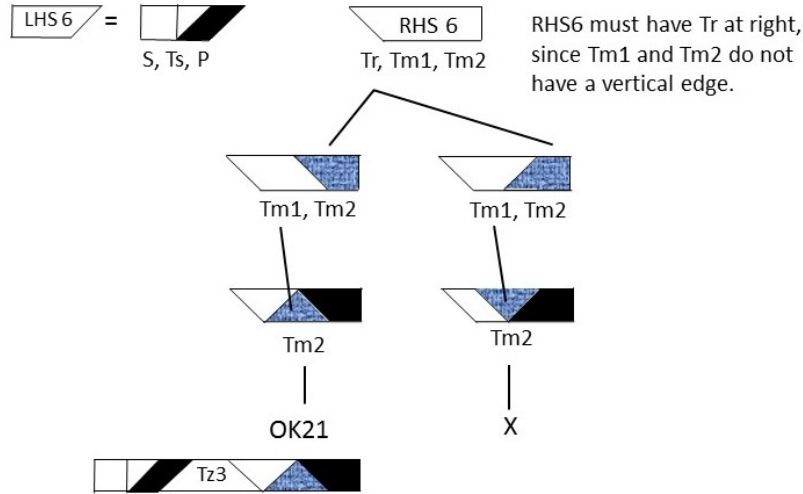


Figure 35: Investigation of the Strip J14\_Tz3.6.

$$\boxed{\text{LHS7}} \diagup \text{Tz3} \diagdown \boxed{\text{RHS7}} \quad \text{with} \quad \boxed{\text{RHS7}} = \begin{array}{c} \diagup \\ \diagdown \end{array} \quad = \{ \text{Tr}, \text{P}, \text{S} \}$$

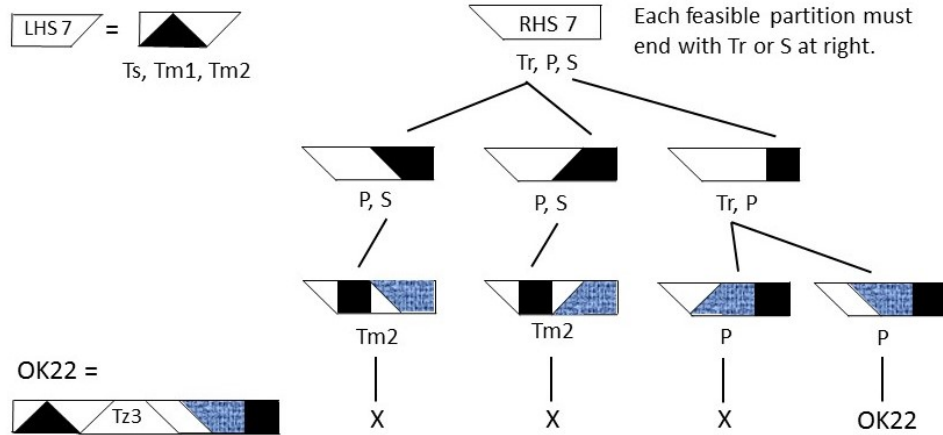


Figure 36: Investigation of the Strip J14\_Tz3.7.

In Fig. 36 we consider case LHS7 consisting of Ts, Tm1 and Tm2. Hence, RHS7 must contain Tr, P and S. Both Tr and S have a vertical edge, so these tans must be placed at right, resulting in 3 partial fillings for RHS. Next we can add S and Tr to these layouts. Notice that after having added S, two tans of type Ts are required for a full filling, but these are not available. Similarly, after having added Tr we find one layout where only Tm can be added while only P is present. The other layout we have to add P and tin this case this is possible, resulting in a feasible layout (denoted by OK22).

Next we have to study the strip with LHS8 with S, Ts and Tm1. Then RHS8 must contain Tr, P and Tm2. Clearly, Tr must be placed at right of RHS8 since P and Tm2 do not have a vertical edge. This gives two options where we can add P, resulting in 4 partial strips. Finally, herein Tm has to be included. This is only possible in two strips. Hence, this case with LHS8 and RHS8 results in 2 feasible partitions for the whole strip. See Fig. 37.

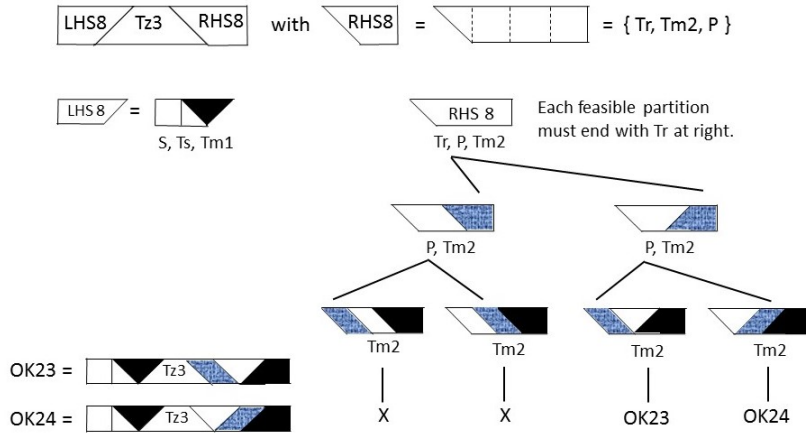


Figure 37: Investigation of the Strip *J14-Tz3.8*.

### 5.2.6 Summary of the analysis of *Strip-J14*

The investigations above for finding all possible partitions of *StripJ14* with the 7 given tans can be summarized by the following steps:

1. Determine all feasible positions and orientations of the isosceles trapezium Tz in strip *J14*, see Fig. 17;
2. Determine all possible partitions for the LHS in the strip, see Figs. 18, 19 and 28;
3. For each of the LHS-partitions: determine all possible layouts for the right hand side (RHS) in the strip using the backtracking principle and being visualized by a tree structure, see Figs. 21 up to 37.

In this way we find all possible partitions of the complete strip *J14*, giving in total 24 different solutions. They are shown in Fig. 38. Moreover, these 24 solutions have also been found by our

computer program (see Fig. 39 and section 6).

For convenience, the equivalence between the partitions (“handmade” and “computer generated”) in both figures is given in Table 1 after Fig. 39. Notice that sometimes we have to apply a horizontal or vertical reflection to a particular partition in Fig. 38 to find the same picture in Fig. 39.

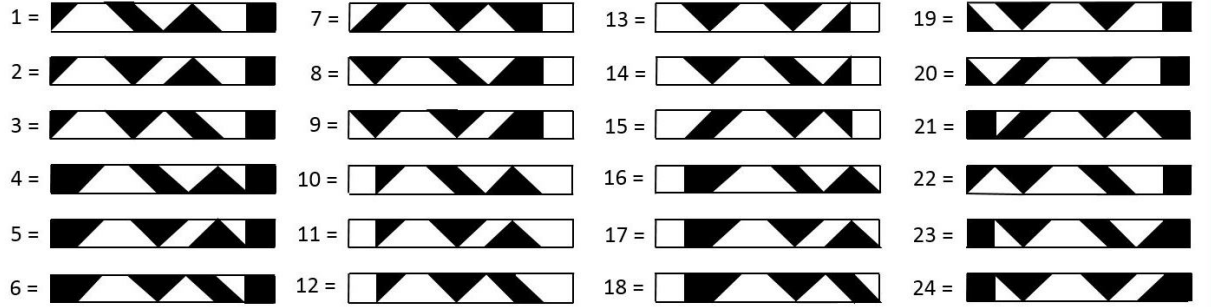


Figure 38: Strip J14 with all its 24 different partitions (“handmade”).

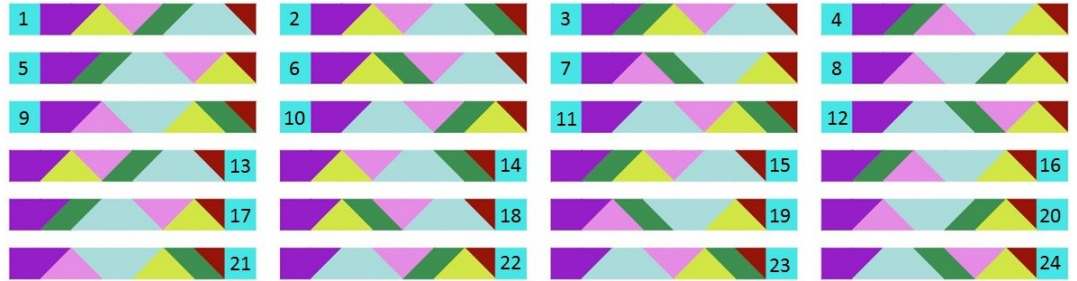


Figure 39: Strip J14 with the 24 partitions (“computer generated”).

Table 1: Correspondence between the handmade and computer generated solutions for Strip J14.

<i>Handmade (part1)</i>	1	2	3	4	5	6	7	8	9	10	11	12
<i>Computer generated</i>	1	6	3	24	22	23	2	7	4	13	18	15
<i>Handmade (part2)</i>	13	14	15	16	17	18	19	20	21	22	23	24
<i>Computer generated</i>	21	20	17	12	10	11	9	8	14	5	19	16

### 5.2.7 Strip J14 with its twin layouts

Let us consider the 24 solutions in Fig.38 in more detail. We can divide each of the strips into the tan S and a 7S-wide substrip L. Notice that S is either at the left or at the right side of the full strip. We will denote the 24 full strips by  $F_1$  up to  $F_{24}$  and their substrips by  $L_1$  up to  $L_{24}$ . Thus, we have either  $F_k = L_k + S$  or  $F_k = S + L_k$  for  $k = 1, \dots, 24$ . The strips  $L_k + S$  and  $S + L_k$  will be called twins and their twin-relationship will be indicated by  $L_k + S \Leftrightarrow S + L_k$ . It is easily seen from Fig. 38 that we have the following twins, shown in Fig. 40.

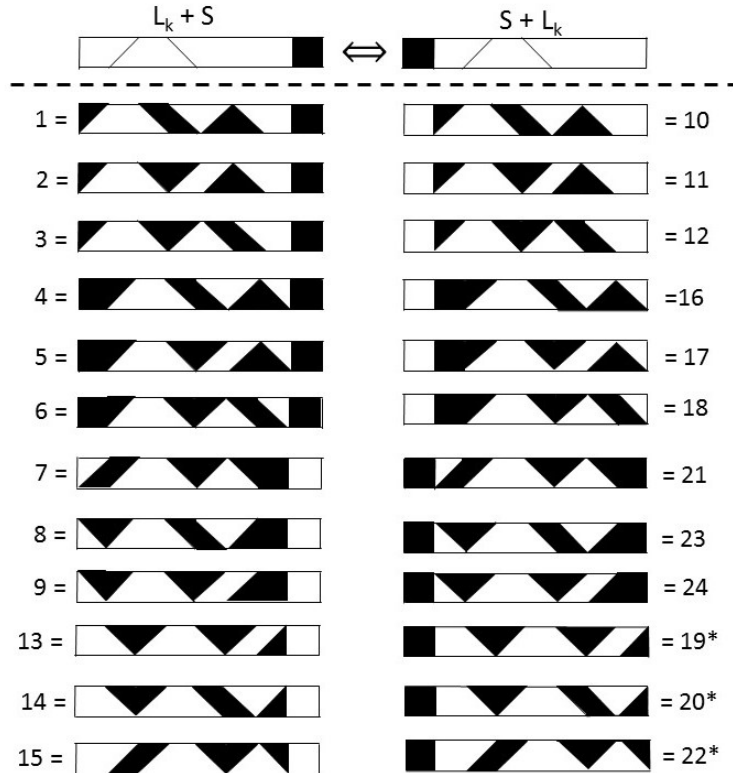


Figure 40: Strip J14 with its 12 twin layouts.

The strips 19\*, 20\* and 22\* are the horizontally flipped strips 19, 20, and 21 in Fig. 38.

### 5.3 Finding all different partitions for $J15$ and $J16$ by a combinatorial approach

We start with considering the structure of all feasible partitions found for the 12 twin pairs in Fig. 40. Notice that inside each of the 24 partitions there are 6 joint edges for each pair of adjacent tans. In particular, precisely 5 of these joint edges are skew, and only one joint (with S) is vertical. We can cut  $J14$  along each of these cutting edges, resulting in 2 separate sub-strips. Next we can reverse the order of these sub-strings and glue them together. Apparently, the latter can be done in two ways (i.e., in original or in upside-down orientation) when the cutting edge is skew.

We will discuss the possible situations for all strips. This is done by using one representative strip. To this end, we can take the first strip  $J14-1$  in Fig. 38.

The cutting edges will be denoted by  $C1$  up to  $C6$ , with  $C6$  being vertical. See Fig. 41.

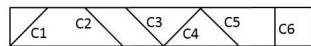


Figure 41: The cuttings edges of strip  $J14-1$ .

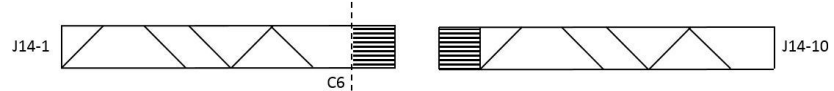


Figure 42: Vertical cutting and pasting of strip  $J14-1$  gives strip  $J14-10$ .

Let us first consider the case with a vertical cutting edge (i.e. the cutting along vertical edge  $C6$  of tan  $S$  inside the strip  $J14-1$ ). This is illustrated in Fig. 42-Left. We obtain the tan  $S$  and a sub-strip of width 7  $S$ . After glueing  $S$  in front of the sub-string we get strip  $J14-10$ , see Fig. 42-Right. It is easily seen that carrying out this process for all strips in the lhs column of Fig. 40 results in the creation of all corresponding twin strips in its rhs column.

Next we consider the case with a skew cutting edge ( $C1$  up to  $C5$ ). The process of “cut and paste” (in two ways) is visualized by the two (representative) examples  $J14-C1$  and  $J14-C2$  in Fig. 43. Then we obtain two new strips, one having the shape of  $J15$ , and the other one that of  $J16$ .

Recalling Fig. 40 we know that  $J14-1$  and  $J14-10$  are twins. We can apply the cut-and-paste process also to twin  $J14-10$ . Now it can easily be easily seen from the examples  $J14-10-C1$  and  $J14-10-C2$  in Fig. 43 that cutting along a skew edge of two strips being twins results in the same strips of type  $J15$  and  $J16$ . Clearly, we can draw the following

**Conclusion:** (10)

**The cut-and-paste process applied to each of the twin pair strips of type  $J14$  in Fig. 40 results in a pair of strips of type  $J15$  and  $J16$ .**

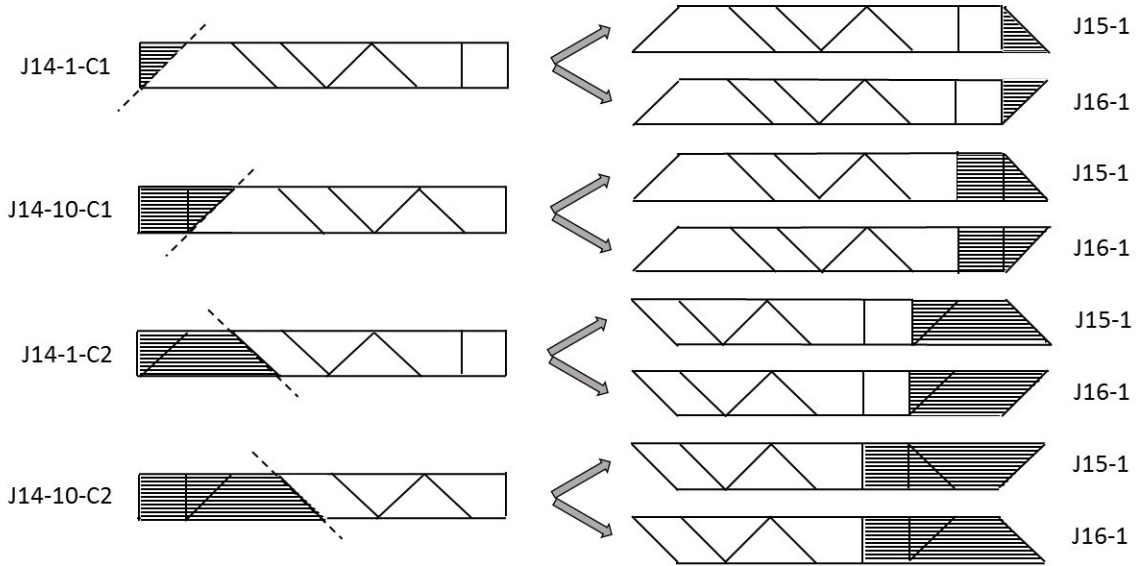


Figure 43: Cutting and pasting the twin strips  $J_{14}$ .

Consequently, we can find precisely 60 different partitions for all  $J_{15}$  as well as  $J_{16}$ -strips, since we have 12 twin pairs of  $J_{14}$ -strips and 5 different skew cutting edges per  $J_{14}$ -strip.

These 60 layouts for both  $J_{15}$  and  $J_{16}$  are shown in the next figures. These layouts are arranged in the following way.

We have 12 groups of layouts, each group is headed by a  $J_{14}$ -layout shown in the lhs column of Fig. 40. These 12 “header”-layouts are labeled by an alphabetical character, ranging from  $A$  to  $L$ . In each group 5 twin pairs consisting of a  $J_{15}$ -layout and its dual  $J_{16}$ -layout are given.

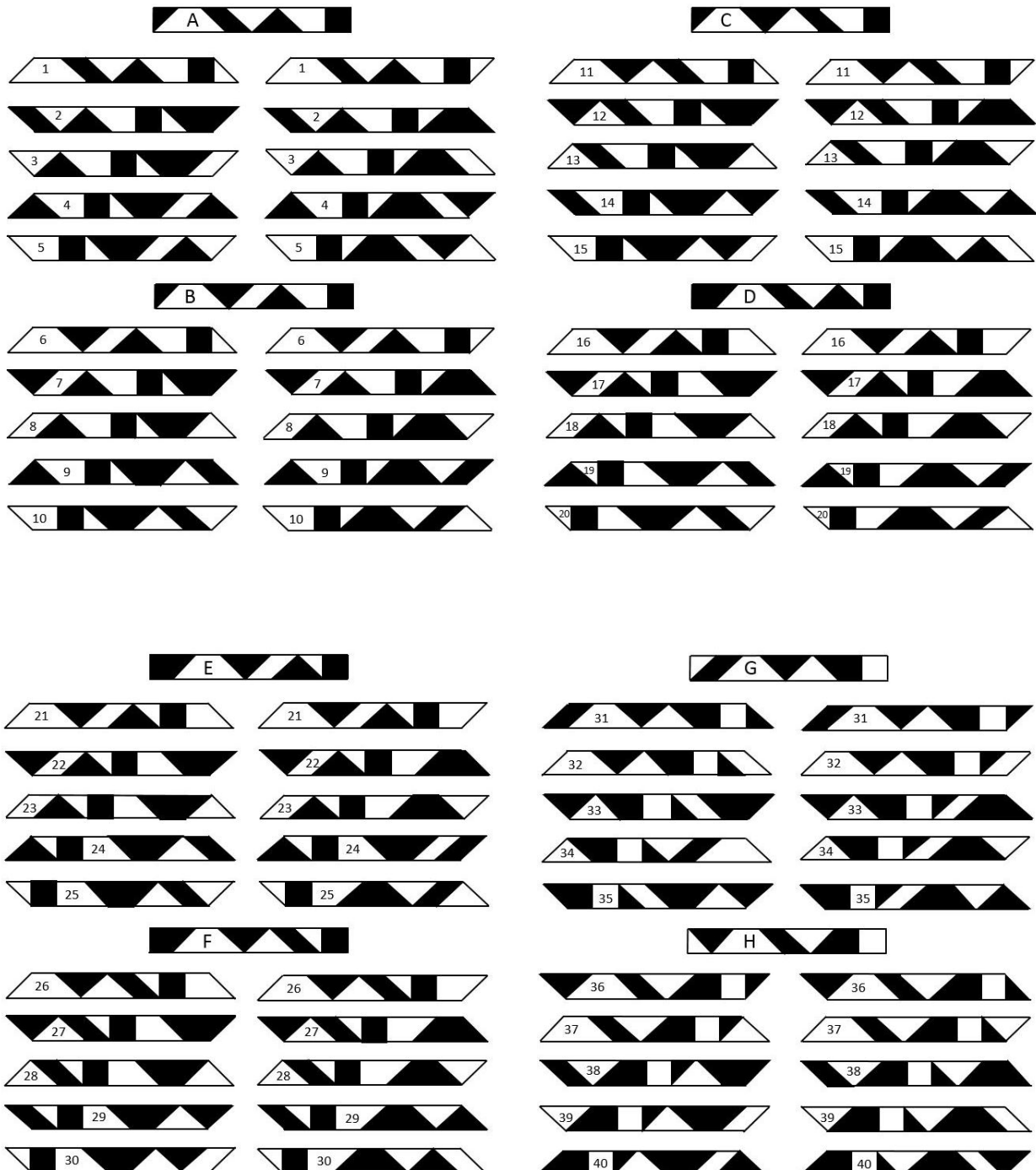


Figure 44: The solutions 1-40 (out of 60) of the strips  $J_{15}$  and  $J_{16}$ .

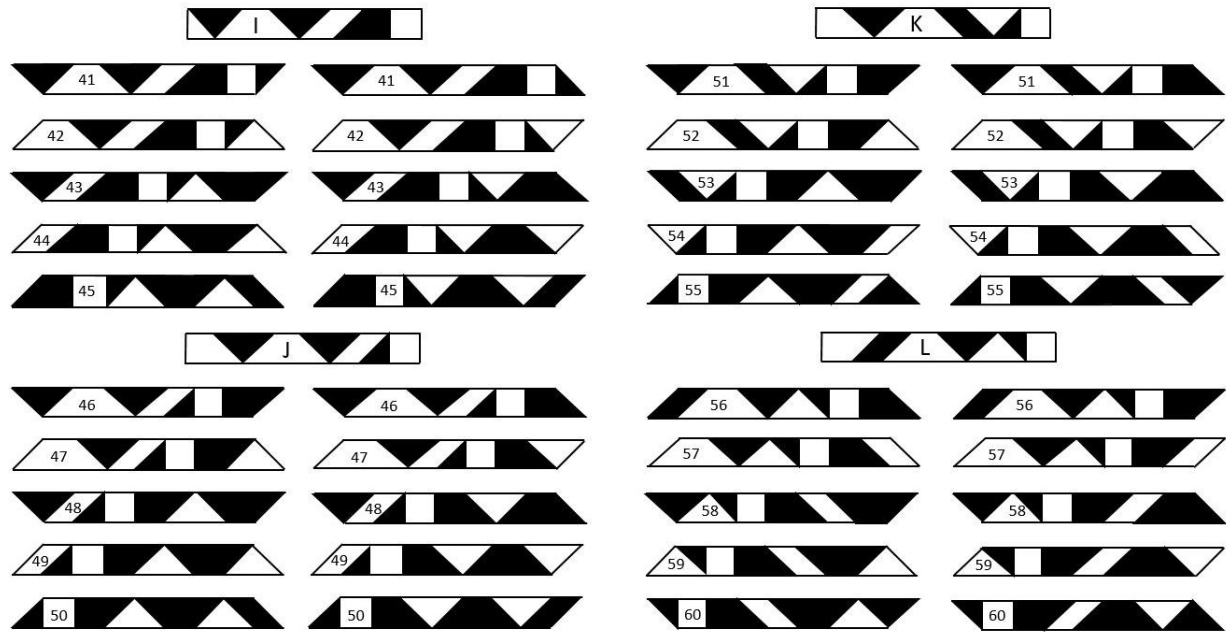


Figure 45: The solutions 41-60 (out of 60) of the strips  $J_{15}$  and  $J_{16}$ .

## 6 An algorithm for generating all partitions of a convex shape

Here we will (globally) explain how the problem of finding all partitions of a convex shape can be solved by a technique used for solving a *packing* problem, see [7]. This will be discussed below. We will first start with a simple packing problem.

### 6.1 A simple packing problem

Let be given a set of simple puzzle pieces and a rectangular box. The problem is to put all pieces in the box, without overlap. For an example, see the *Simple Puzzle* in Fig. 46 with a *box* with  $2 \times 3$  unit *cells* and the 3 *pieces* *A*, *B* and *C*.

We introduce the notions *Aspect* and *Embedding*:

*Aspect*: the cell in the box, the type of a piece.

*Embedding*: the placement of a piece in the box can be encoded by a set of *aspects*.

In our example we have  $\text{Aspects} = \{0, 1, \dots, 5, A, B, C\}$  and the *Embeddings* are given by Fig. 47. Note that a solution to such a packing puzzle consists of a set of embeddings constituting a partition of the set of aspects; that is, the embeddings in a solution are pairwise disjoint.

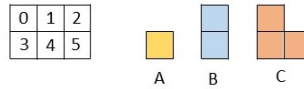


Figure 46: The box with  $2 \times 3$  cells and the 3 puzzle pieces *A*, *B* and *C*.

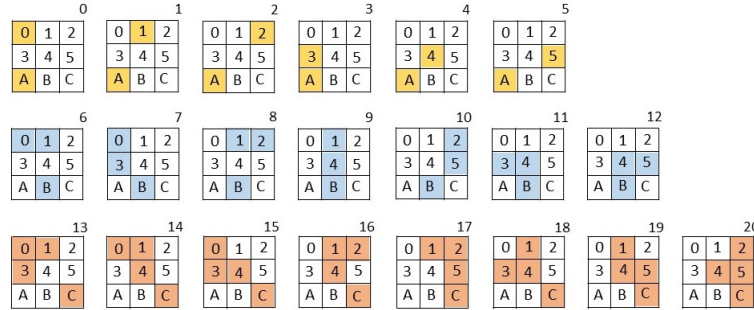


Figure 47: The Aspects and Embeddings of a simple puzzle.

It is important (for performance) that we eliminate symmetries (if any). This can be done by *restricting* the embeddings. We will illustrate this by an example. To this end, consider the previous example, where we will restrict piece *C* to be the *horizontally mirrored* letter L. We call

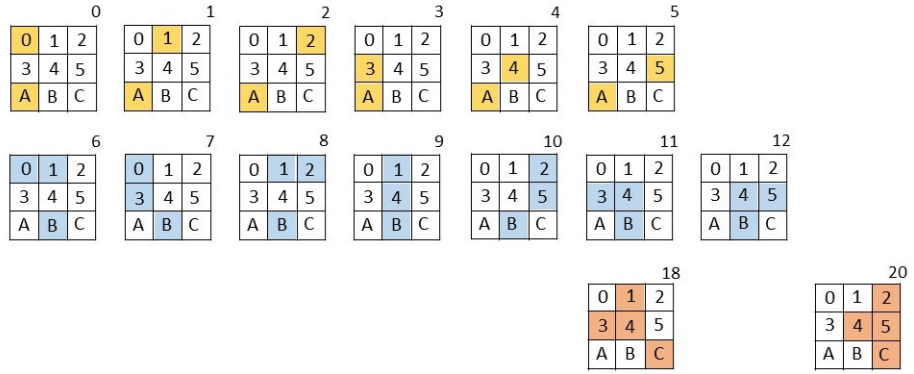


Figure 48: Eliminating symmetries by restricting embeddings.

this example *Simple L-restricted Puzzle*. This results in the embeddings in Fig. 48. It can easily be seen that the following 3 sets of embeddings  $E_1, E_2, E_3$  solve this puzzle, where

$$E_1 = \{0, 10, 18\}, \quad E_2 = \{1, 7, 20\} \quad \text{and} \quad E_3 = \{3, 6, 20\}. \quad \text{See also Fig. 49.}$$

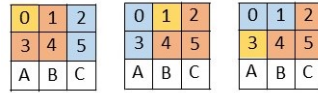


Figure 49: The 3 embeddings that solve the *Simple L-restricted Puzzle*.

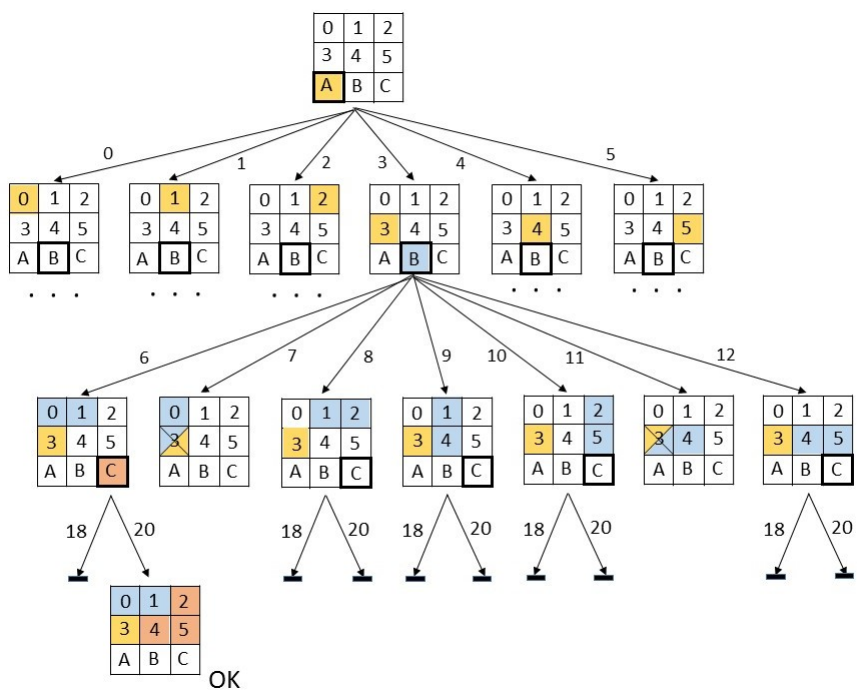


Figure 50: The backtracking tree for solving the *Simple L-restricted Puzzle*, with the embeddings  $\{3, 6, 20\}$  as solution.

Clearly, when dealing with a more complex puzzle we in general cannot easily find its solution(s) by hand. Then we might try to solve the puzzle using a computer and a dedicated solving procedure such as *backtracking*, see [8], [9]. Recall that the *search tree* is an important concept for the backtracking method. This is a graphical representation of all possible cases to be studied for finding a solution. In Fig. 50 we show (a part of) the search tree corresponding to the *Simple L-restricted Puzzle*.

## 6.2 A more complicated packing problem

Now we want to consider a more complicated packing problem which is related to the problem of finding all partitions of each of the convex shapes using the Japanese set of tans.

Recalling Conclusion (v) in (2) and Fig. 2 in section 2 we know that each convex shape formed by the 7 Japanese tans consists of 16 isosceles rectangular triangles  $Ts$ . Next we can split each  $Ts$  into two smaller triangles  $ts$ , i.e.,  $ts = Ts/2$ . So, the complete set of tans can be built up with 32 triangles  $ts$ , see Fig. 51. Now consider a rectangular box with 8 square cells, each of them being

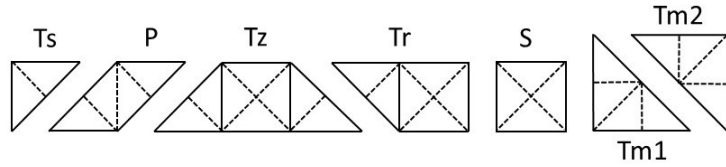


Figure 51: Subdividing all Japanese tans into triangles  $ts$ , with  $ts = Ts/2$ .

divided into 4 isosceles rectangular triangles  $ts$ . See Fig. 52.

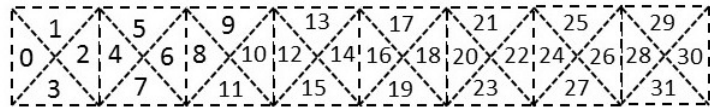


Figure 52: Box with 8 cells, each being subdivided into 4 triangles  $ts$ .

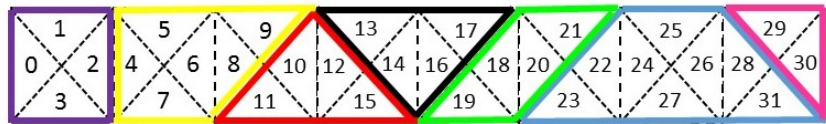


Figure 53: The box in Fig. 52 being fully covered by a partition of the strip  $J14$ .

This suggests that the 7 tans can fully fill this box. Indeed, a possible filling is given in Fig. 53.

### 6.2.1 The packing problem for Strip J14

Notice that in fact Fig. 53 shows a partition of strip J14, see also Fig. ??.

The situation in Fig. 53 is similar to that for the *Simple L-restricted Puzzle*. So, similar to Fig. 50 for this puzzle we can also use the backtracing algorithm to find all different partitions of J14.

### 6.2.2 The packing problem for Strip J16

Next, let us consider the parallelogram-shaped strip J16 (recall Fig. ??).

It is easily seen that the partition of J14 in Fig. 53 can be transformed to a partition of J16 by moving the triangle  $\{29, 30\}$  at the most right side to the most left side. Of course, this partition of J16 fits (partially) in a *larger* 1x9 rectangular box. See Fig. 54.

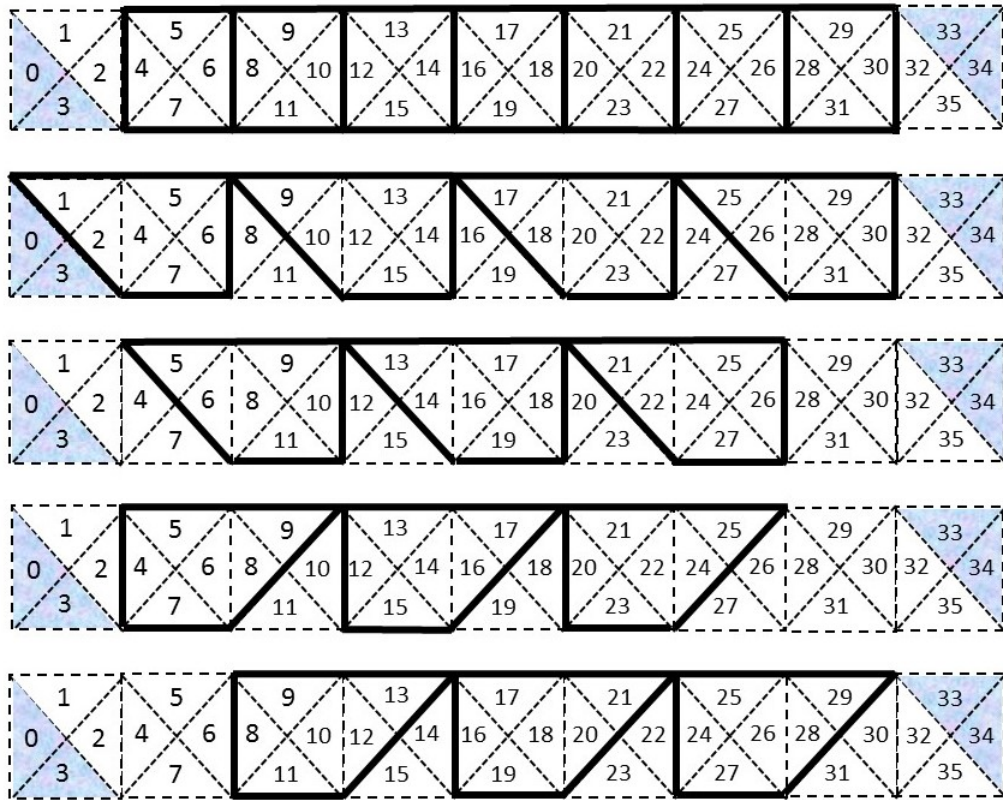


Figure 54: The enlarged box being (partially) covered by a partition of the strip J16.

Just as for the example *Simple L-restricted Puzzle* we can now establish the embeddings for each individual tan in the box in Fig. 54. Notice that in order to find all essentially different partitions we have to take into account all possible orientations of each tan when establishing the embeddings. We will illustrate this for two tans (*S* and *Tr*) only. The remaining tans can be described in a similar way.

Using Fig. 54 we find the following embeddings:

- $S$  in row 1:  $\{4, 5, 6, 7\}, \{8, 9, 10, 11\}, \dots, \{28, 29, 30, 31\}$
- $Tr$  in row 2:  $\{1, 2, 4, 5, 6, 7\}, \{9, 10, 12, 13, 14, 15\}, \{17, 18, 20, 21, 22, 23\}, \{25, 26, 28, 29, 30, 31\}$
- $Tr$  in row 3:  $\{5, 6, 8, 9, 10, 11\}, \{13, 14, 16, 17, 18, 19\}, \{21, 22, 24, 25, 26, 27\}$
- $Tr$  in row 4:  $\{4, 5, 6, 7, 8, 9\}, \{12, 13, 14, 15, 16, 17\}, \{20, 21, 22, 23, 24, 25\}$
- $Tr$  in row 5:  $\{8, 9, 10, 11, 12, 13\}, \{16, 17, 18, 19, 20, 21\}, \{24, 25, 26, 27, 28, 29\}.$

Once having established all embeddings for all tans, we determine all possible partitions of the strip  $J16$  by using a backtracking algorithm, completely similar to example *Simple L-restricted Puzzle*.

#### **Remarks :**

- The establishment of the embeddings and the backtracking can be automatically generated by a dedicated computer program.
- Clearly, we can use the approach described above for *all* 16 convex polygons in Fig. ??-Right that can be formed by the set of the Japanese tans. Of course, we need a box of  $m \times n$  square cells for the polygons  $J1$  up to  $J13$ , with  $m$  and  $n$  such that the polygon under study fits in this box.
- In case we have two tans with the same shape but with different colour, then interchanging them in a layout gives a different partition, in contrast to the monochromatic case. This situation needs special attention when using a computer program for finding all different partitions.

In the next section we show all possible partitions of the mentioned 16 convex polygons.

## 7 All different partitions of the shapes $J01$ up to $J16$

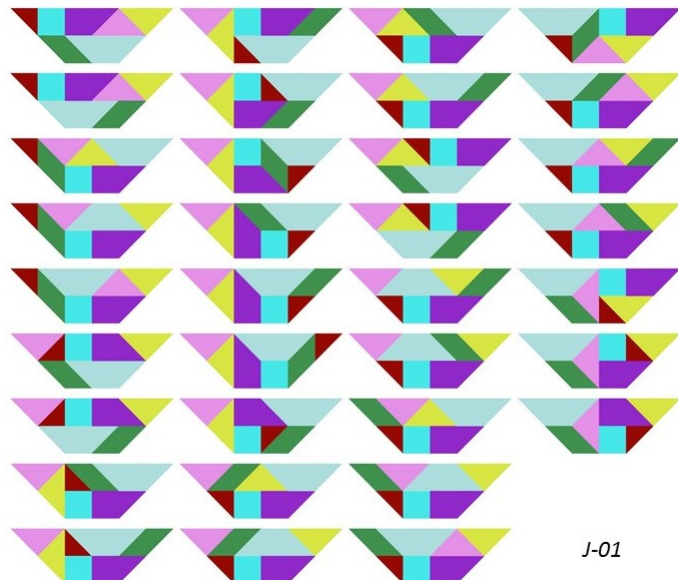


Figure 55: All 34 different layouts of shape  $J01$ .

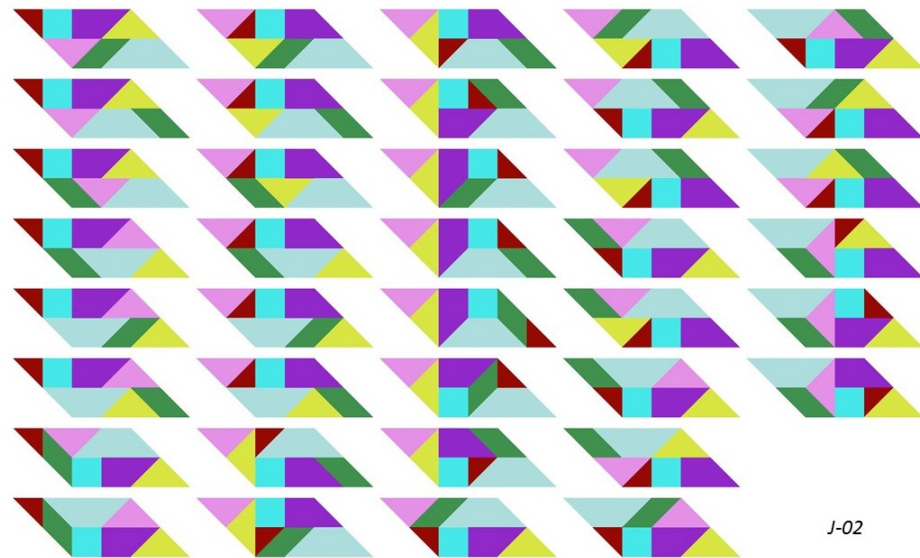
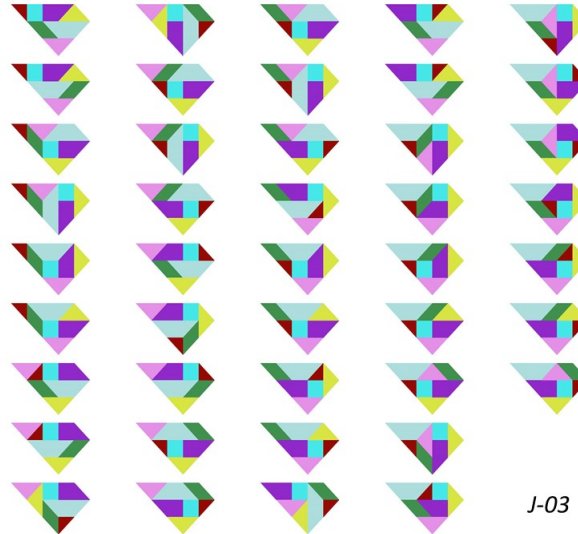
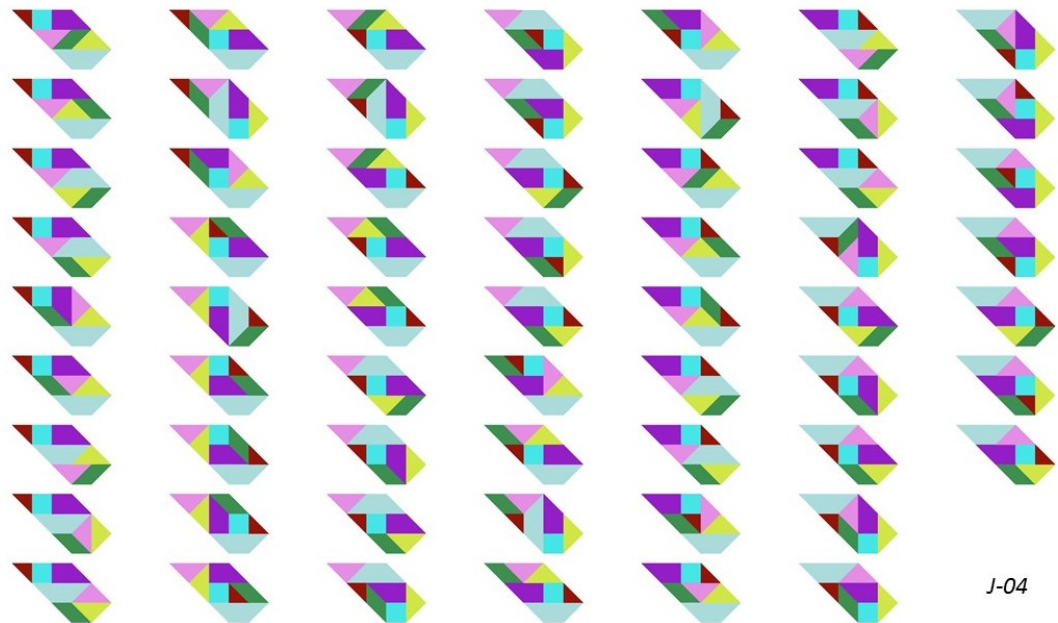


Figure 56: All 38 different layouts of shape  $J02$ .



J-03

Figure 57: All 43 different layouts of shape J03.



J-04

Figure 58: All 61 different layouts of shape J04.

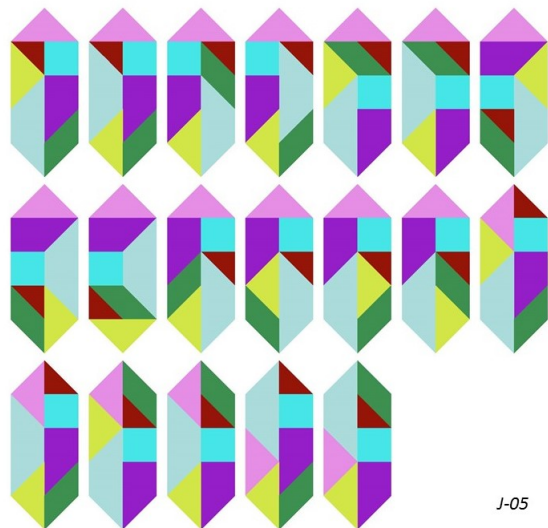


Figure 59: All 19 different layouts of shape  $J05$ .

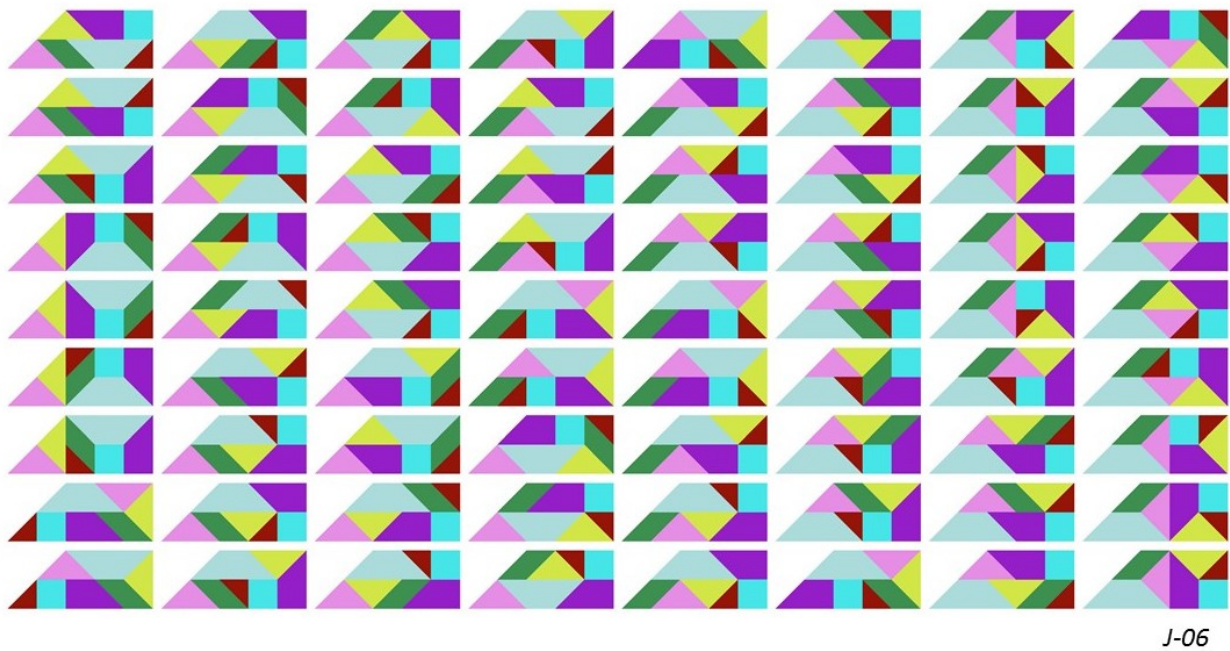
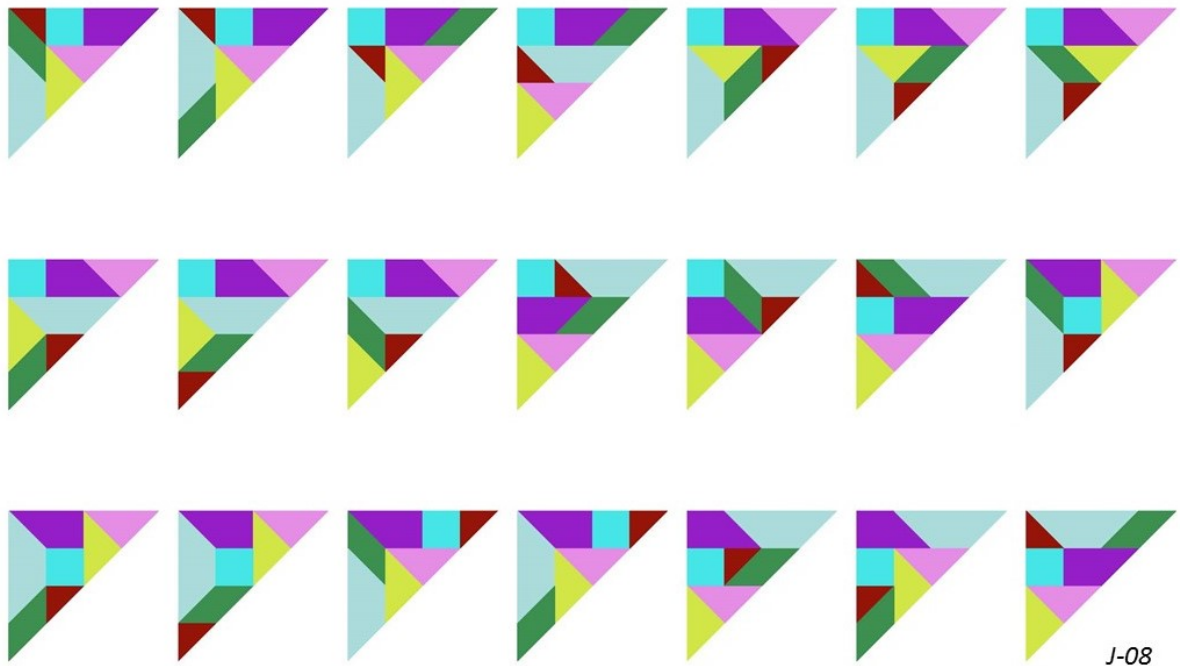


Figure 60: All 72 different layouts of shape  $J06$ .



J-07

Figure 61: All 3 different layouts of shape J07.



J-08

Figure 62: All 21 different layouts of shape J08.

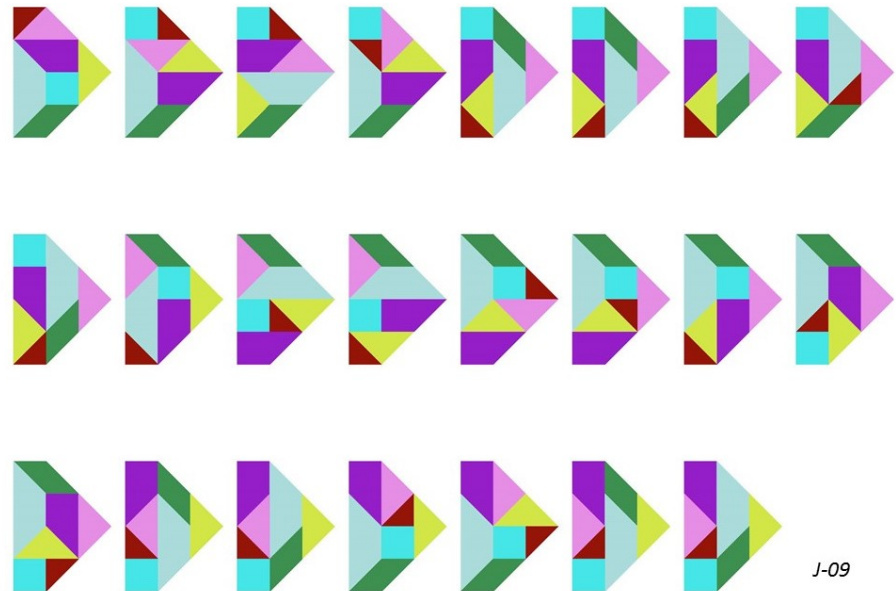


Figure 63: All 23 different layouts of shape J09.

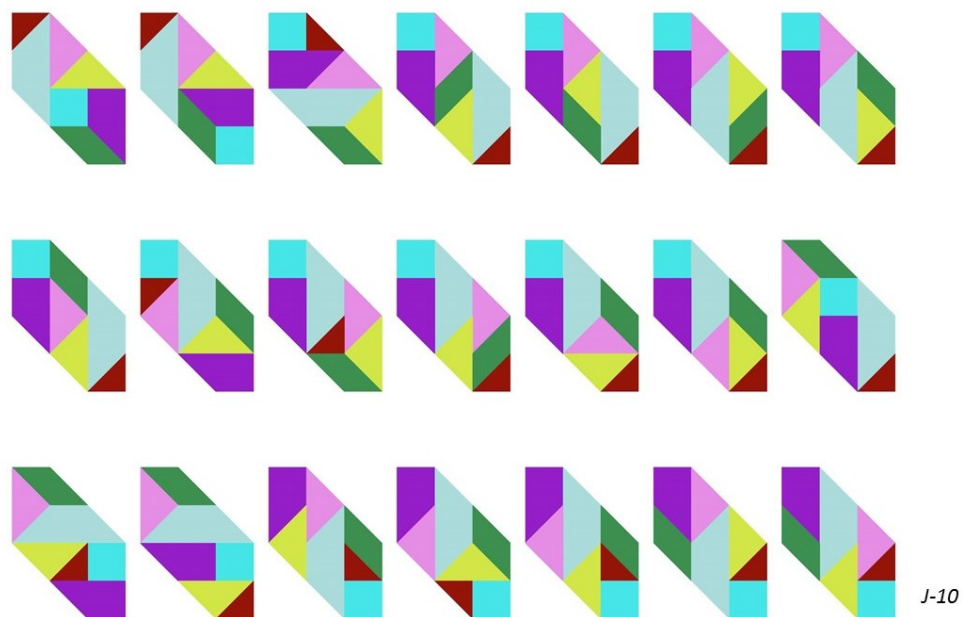


Figure 64: All 21 different layouts of shape J10.

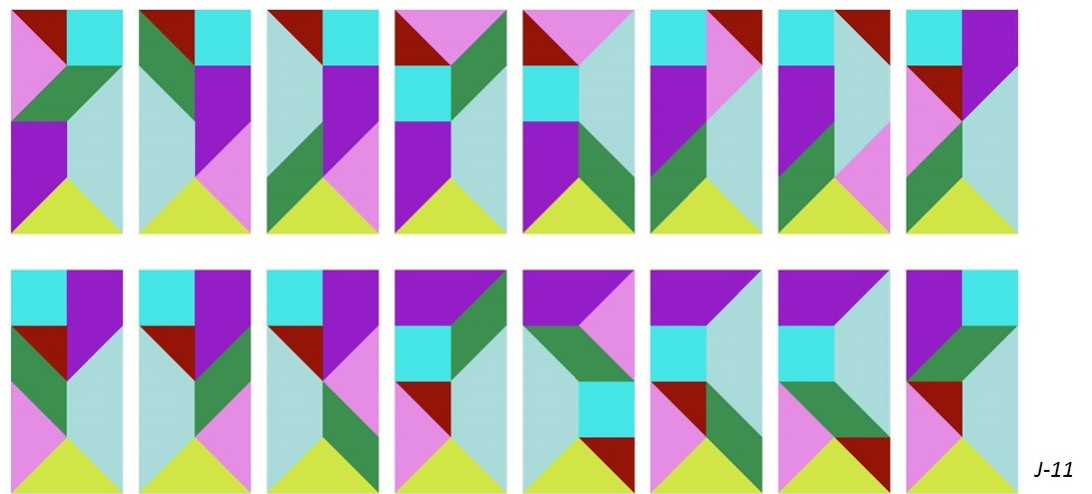


Figure 65: All 16 different layouts of shape *J*11.

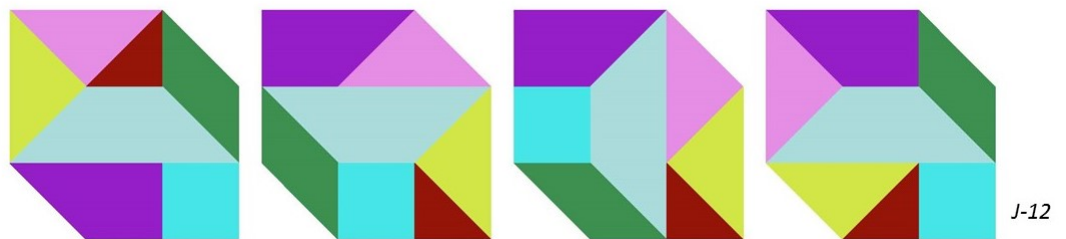


Figure 66: All 4 different layouts of shape *J*12.

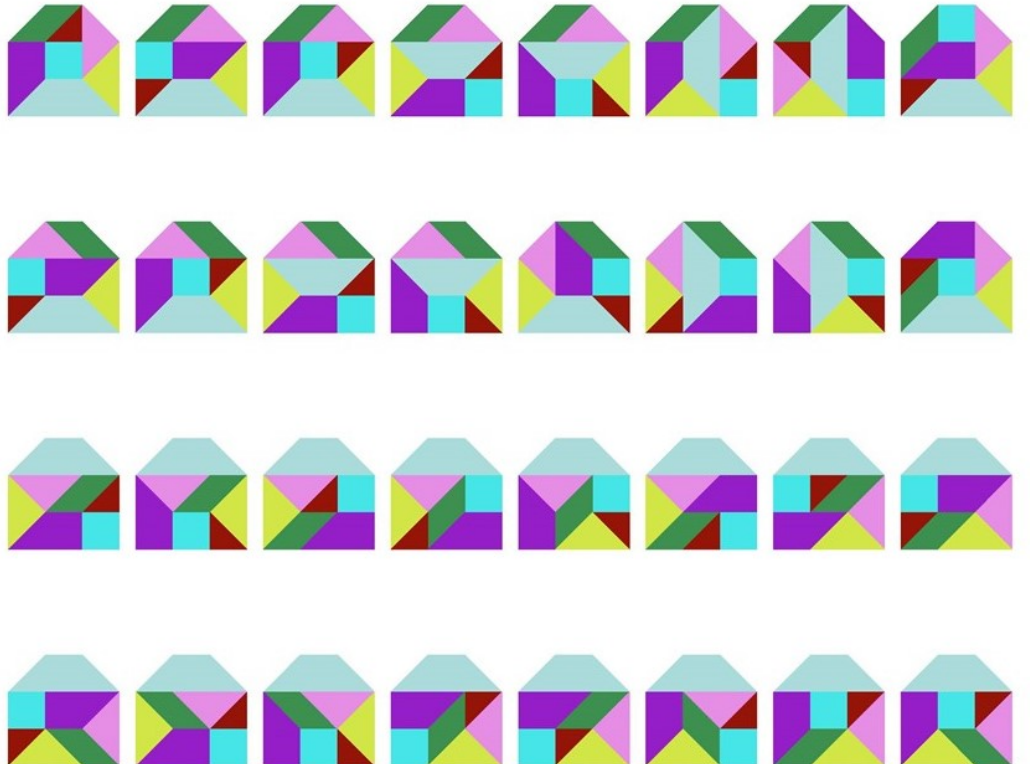


Figure 67: All 32 different layouts of shape J13.

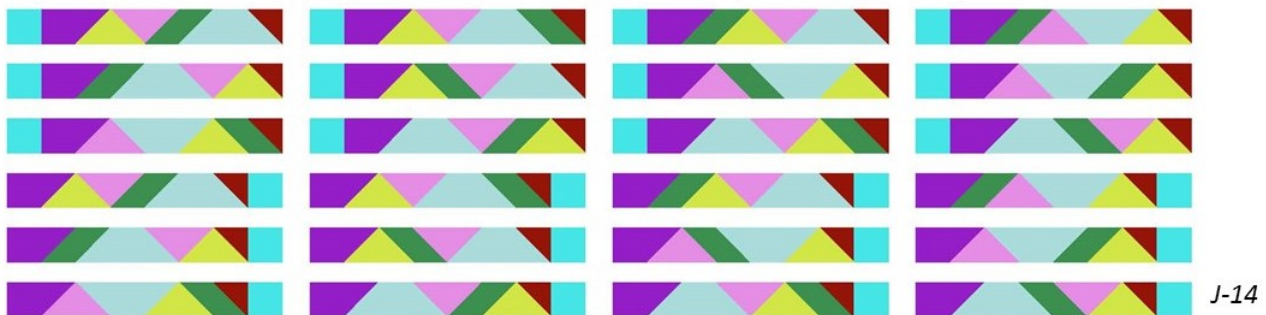


Figure 68: All 24 different layouts of shape J14.

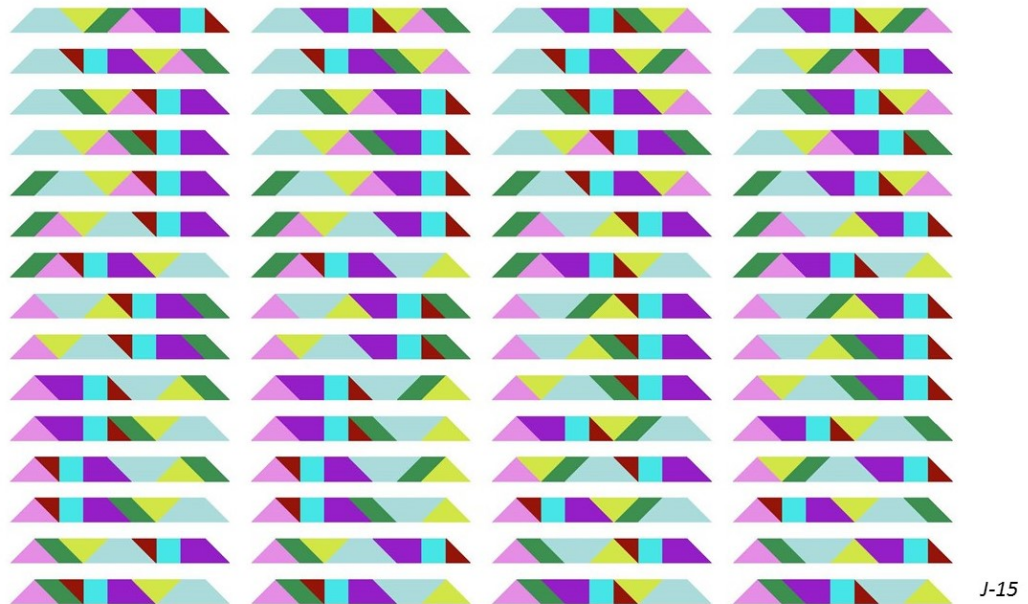


Figure 69: All 60 different layouts of shape  $J15$ .

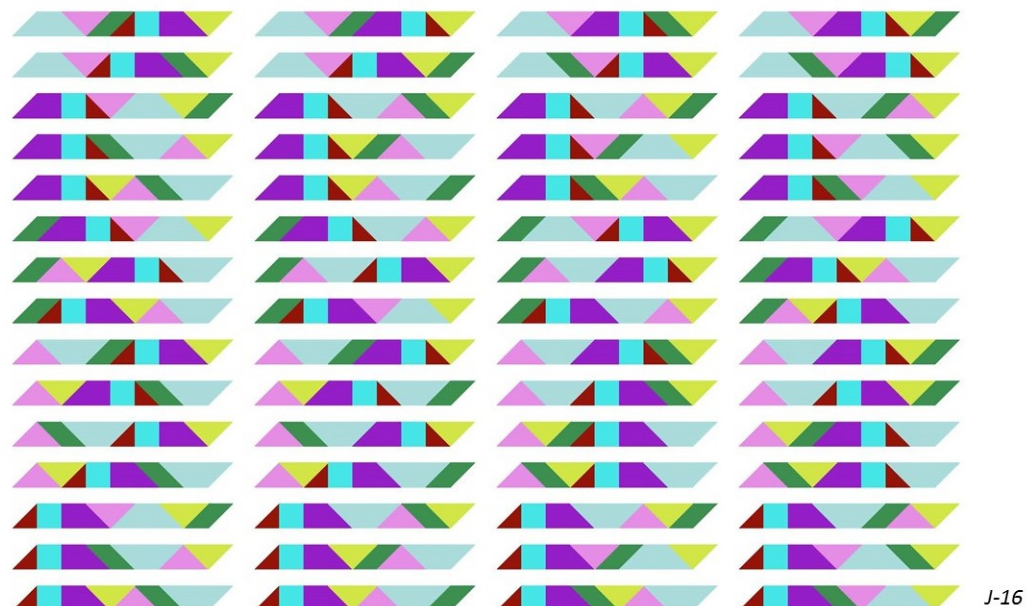


Figure 70: All 60 different layouts of shape  $J16$ .

Table 2: Summary: Number of different partitions per shape.

<i>Shape</i>	1	2	3	4	5	6	7	8	9	10	11	12	13	14	15	16
<i># partitions</i>	34	38	43	61	19	72	3	21	23	21	16	4	32	24	60	60

## 8 Acknowledgments and References

### Acknowledgments

The author wishes to thank co-author Tom Verhoeff for his stimulating discussions and for providing and running his dedicated software to generate all solutions we were looking for. Without his help the results as presented in this report would not have been found.

Last but not least I would like to express my appreciation to Mrs. Hui Jun Chang who read this report carefully and gave several valuable suggestions for improvement.

### References

- [1] Fu Traing Wang, Chuan-Chih Hsiung, *A Theorem on the Tangram*, The American Mathematical Monthly, Vol. 49, No. 9, 1942, pp. 596-599, available at <http://www.jstor.org/stable/2303340>.
- [2] Joost Elffers, *Tangram, Das alte chinesische Formenspiel / Het oude Chinese vormenspel*, M. DuMont Schauberg, Cologne, 1976, 3rd edition.
- [3] T.G.J. Beelen, *Finding all convex tangrams*, Eindhoven University of Technology, CASA-report 17-02, 2017.
- [4] T.G.J. Beelen, *Determining the essentially different partitions of all Chinese convex tangrams*, Eindhoven University of Technology, CASA-report 18-02, 2018.
- [5] T.G.J. Beelen, T. Verhoeff, *Determining the essentially different partitions of all Japanese convex tangrams*, Eindhoven University of Technology, CASA-report 18-07, 2018.
- [6] <http://www.pentoma.de/>, Tangram Uebersicht, Konvexe Figuren, 2017.
- [7] Erik van der Tol and Tom Verhoeff, *The Puzzle Processor Project: Towards an Implementation*, Nat. Lab. Unclassified Report NL-UR 2000/828, Koninklijke Philips Electronics N.V., 2001.
- [8] <https://en.wikipedia.org/wiki/Backtracking/>, Description of the (backtracking) method, 2017.
- [9] <https://www.geeksforgeeks.org/backtracking/>, 2017.
- [10] Eli Fox-Epstein, Ryuhei Uehara, *The Convex Configurations of “Sei Shonagon Chie no Ita”*, and Other Dissection Puzzles, arXiv:1407.1923v1, July 2014.